

A non-universal $U(1)_X$ extension to the Standard Model to study the B meson anomaly and muon $g - 2$

J. S. Alvarado^{1,*}, S. F. Mantilla^{2,†}, R. Martinez^{1,‡} and F. Ochoa^{1,§}

¹*Departamento de Física, Universidad Nacional de Colombia,
Ciudad Universitaria, K. 45 No. 26-85, Bogotá D.C., Colombia and*

²*Max-Planck Institute for the Physics of Complex Systems, D-01187 Dresden, Germany*
(Dated: September 8, 2021)

We study an abelian $U(1)_X$ extension to the Standard Model group consisting of an extended scalar sector of two doublets and one singlet plus three additional exotic quarks and two exotic leptons through non-universal interaction of the new X quantum number and a \mathbb{Z}_2 parity. In this model, the lightest fermions are massless at tree-level so effective operators up to dimension seven are considered to fill all zeros in mass matrices, providing an upper bound for the Λ energy scale from the electron, up, down and strange quark masses. We obtain that the model can explain the B meson anomaly while it provides an upper bound for v_χ of 8.4 TeV which translates in an upper bound for the new Z_2^μ gauge boson of 9.9 TeV. Finally, muon $g - 2$ contributions are also studied, where we found that positive contributions coming from charged W^+ bosons and exotic Majorana neutrinos while contributions coming from heavy charged and neutral scalar bosons, are negative. In particular, the allowed regions according to the experimental muon $g - 2$ parameter, shows that as the exotic neutrino mass increases, heavy scalars and the exotic lepton masses increase as well.

* jsalvaradog@unal.edu.co

† mantilla@pks.mpg.de

‡ remartinezm@unal.edu.co

§ faochoap@unal.edu.co

I. INTRODUCTION

Several extensions to the Standard Model (SM) have arisen in an attempt to explain neutrino masses, the muon $(g-2)_\mu$ anomaly among other promising experimental results. Some of these extensions consider additional scalar doublets and singlets which translates in the existence of charged scalars and pseudoscalars, additional heavy fermion singlets such as right-handed and Majorana neutrinos to explain neutrino masses through seesaw mechanisms [1]. Up to date, there is a lower bound for the charged scalar mass in the range 570 – 800 GeV for the 2HDM according to the B meson decays [2] while for exotic leptons, vectorlike lepton masses in the range 114 – 176 GeV are mostly excluded, as reported by the ATLAS collaboration [3]. In relation to the muon anomalous magnetic moment, the muon $g-2$ experiment at Fermilab has recently reported a deviation Δa_μ from the SM prediction of [4]:

$$\Delta a_\mu = a_\mu^{exp} - a_\mu^{SM} = (251 \pm 59) \times 10^{-11}, \quad (1)$$

which represents at 4.2σ deviation from the SM [4] in combination with the Brookhaven National Laboratory (BNL)[5]. an important precision improvement is expected in the near future by experiments as Fermilab E989 [6], which expects to measure nearly a 5σ deviation, and similarly by J-PARC [7]. In addition, this $a_\mu = \frac{g_\mu-2}{2}$ anomaly is a promising result for new physics beyond the Standard Model which has motivated several models to explain it. For instance, it can be done by considering flavor changing processes as a consequence of higher symmetry groups such as 331 models [8], two Higgs doublet models [9], $L_\mu - L_\tau$ $U(1)$ symmetry models [10, 11], $U(1)$ extensions [12] among other new physics scenarios [13]. On the other hand, the rare semi-leptonic decays of B -meson is a promising scenario for leptonic flavor universality violation. A relative branching fraction $R_K^{exp} = \mathcal{B}(B \rightarrow K\mu^+\mu^-)/\mathcal{B}(B \rightarrow Ke^+e^-) = 0.846_{-0.041}^{+0.044}$ at 3.1σ [14] has been recently reported by the LHCb collaboration, $R_{K^*} = 0.69_{-0.07}^{+0.11} \pm 0.05$ at 2.4σ by the LHCb collaboration as well [15], both in the interval $1.1 \text{ GeV}^2 < q^2 \leq 6 \text{ GeV}^2$, and the most recent world average for the B_s branching ratio $\mathcal{B}[B_s \rightarrow \mu^+\mu^-]_{exp} = (2.93 \pm 0.35) \times 10^{-9}$ at 2.3σ [16] compared to the Standard Model (SM) prediction $\mathcal{B}[B_s \rightarrow \mu^+\mu^-]_{SM} = (3.66 \pm 0.14) \times 10^{-9}$ [17], which certainly shows a discrepancy. Such important measurement improvement of R_K is an indicator of possible physics beyond the standard model such as new non-universal interactions [18], flavor dependent Z' models in abelian and non-abelian extensions [19], supersymmetry [20], leptoquarks [21] among others.

Another interesting scenario to address these experimental anomalies is effective field theory, which is a useful method to incorporate the high energy physics effects into the lower energy scale by “integrating out” the heavy degrees of freedom, which lead us to an effective Lagrangian as a dimensional expansion

$$\mathcal{L} = \mathcal{L}_0 + \frac{\mathcal{L}_1}{\Lambda} + \frac{\mathcal{L}_2}{\Lambda^2} + \dots, \quad (2)$$

where \mathcal{L}_0 contains all renormalizable interactions while \mathcal{L}_n , with $n \geq 1$, is a combination of non-renormalizable operators of dimension $n+4$ suppressed by powers of the new physics energy scale Λ^n , in all cases restricted by gauge symmetry. Roughly speaking, it makes renormalizability to be understood as the requirement that low energy physics cannot dramatically depend on the physics at higher scales [22]. These effective operators encode loop processes that can be measured at a low energy scale such as magnetic and electric dipole moments ($\bar{\psi}\sigma_{\mu\nu}\psi F^{\mu\nu}$ [23], $\bar{\psi}\sigma_{\mu\nu}\gamma^5\psi F^{\mu\nu}$ [24]), the Higgs to diphoton decay ($hF_{\mu\nu}^a F^{a\mu\nu}$) [25], particle masses [26] among others, which in general are sensitive to new physics. In particular, certain mass matrix textures implies massless particles which are identified as the lightest fermions whose mass is justified by loop processes. Instead, we can consider higher dimensional operators, allowed by the symmetries of the model to explain the masses of the lightest fermions such as the electron and the quarks up, down and strange.

In this work, we first give an overview of the abelian extension in section II, then masses and rotation matrices for scalars, gauge bosons, leptons and quarks are introduced in sections III, IV V and VI respectively, where effective operators have been considered to explain the masses of the lightest fermions. Later, we study the effect of the new particles in the B meson anomaly in section VII and Muon $g-2$ in section VIII. Finally, some conclusions are discussed in section IX.

II. THE $U(1)_X$ EXTENSION

The proposed abelian extension $\mathcal{G}_{SM} \otimes U(1)_X$ to the SM is made out of two scalar doublets, with identical hypercharge but different X quantum number and \mathbb{Z}_2 parity, responsible for electroweak symmetry breakdown, and

one scalar singlet whose Vacuum Expectation Value (VEV) at a higher energy scale is responsible of the $U(1)_X$ spontaneous symmetry breaking (SSB) as shown in Table I.

Scalar Doublets			Scalar Singlets		
	X^\pm	Y		X^\pm	Y
$\phi_1 = \begin{pmatrix} \phi_1^+ \\ \frac{h_1+v_1+i\eta_1}{\sqrt{2}} \end{pmatrix}$	$+2/3^+$	$+1$	$\chi = \frac{\xi_\chi+v_\chi+i\zeta_\chi}{\sqrt{2}}$	$-1/3^+$	0
$\phi_2 = \begin{pmatrix} \phi_2^+ \\ \frac{h_2+v_2+i\eta_2}{\sqrt{2}} \end{pmatrix}$	$+1/3^-$	$+1$			

TABLE I: Scalar particle content of the model, X -charge, \mathbb{Z}_2 parity and hypercharge.

On the other hand, the fermionic sector is based on a non-universal $X \otimes \mathbb{Z}_2$ charge assignation among the three SM generations plus some additional exotic singlet particles. The quark sector considers one exotic up-like quark \mathcal{T} while there are additional two down-like particles $\mathcal{J}^{1,2}$. Likewise, there are two exotic lepton singlets E and \mathcal{E} , three right-handed neutrinos ν_R and three Majorana neutrinos \mathcal{N}_R intended to provide the active neutrino masses as shown in table II. Besides, the following notation is used for the flavor states:

$$\begin{aligned}
 U^{1,2,3} &= (u, c, t), & D^{1,2,3} &= (d, s, b), \\
 e^{e,\mu,\tau} &= (e, \mu, \tau), & \nu^{e,\mu,\tau} &= (\nu^e, \nu^\mu, \nu^\tau).
 \end{aligned}$$

Quarks	X	\mathbb{Z}_2	Leptons	X	\mathbb{Z}_2
$q_L^1 = \begin{pmatrix} u^1 \\ d^1 \end{pmatrix}_L$	$+1/3$	$+$	$\ell_L^e = \begin{pmatrix} \nu^e \\ e^e \end{pmatrix}_L$	0	$+$
$q_L^2 = \begin{pmatrix} u^2 \\ d^2 \end{pmatrix}_L$	0	$-$	$\ell_L^\mu = \begin{pmatrix} \nu^\mu \\ e^\mu \end{pmatrix}_L$	0	$+$
$q_L^3 = \begin{pmatrix} u^3 \\ d^3 \end{pmatrix}_L$	0	$+$	$\ell_L^\tau = \begin{pmatrix} \nu^\tau \\ e^\tau \end{pmatrix}_L$	-1	$+$
$U_R^{1,3}$	$+2/3$	$+$	$e_R^{e,\tau}$	$-4/3$	$-$
U_R^2	$+2/3$	$-$	e_R^μ	$-1/3$	$-$
$D_R^{1,2,3}$	$-1/3$	$-$			
Non-SM Quarks			Non-SM Leptons		
T_L	$+1/3$	$-$	$\nu_R^{e,\mu,\tau}$	$1/3$	$-$
T_R	$+2/3$	$-$	$N_R^{e,\mu,\tau}$	0	$-$
$J_L^{1,2}$	0	$+$	E_L, \mathcal{E}_R	-1	$+$
$J_R^{1,2}$	$-1/3$	$+$	\mathcal{E}_L, E_R	$-2/3$	$+$

TABLE II: Fermion particle content of the model, X -charge, \mathbb{Z}_2 parity and hypercharge.

The exotic singlet VEV, v_χ , breaks the $U(1)_X$ symmetry of the model into the SM group. Such an energy scale is expected to be at the TeV scale and as it is shown in section IV, it provides mass to the Z' gauge boson. Besides, the non-universal assignation generates suitable mass matrix textures which can explain the fermion mass hierarchy, while exotic particles are mainly dependent on the v_χ scale and arise from the requirement of a chiral anomaly free theory, setting the following equations to zero:

$$\begin{aligned}
[\text{SU}(3)_C]^2 \text{U}(1)_X &\rightarrow A_C = \sum_Q [X_{Q_L} - X_{Q_R}] \\
[\text{SU}(2)_L]^2 \text{U}(1)_X &\rightarrow A_L = \sum_\ell [X_{\ell_L} + 3X_{Q_L}] \\
[\text{U}(1)_Y]^2 \text{U}(1)_X &\rightarrow A_{Y^2} = \sum_{\ell, Q} [Y_{\ell_L}^2 X_{\ell_L} + 3Y_{Q_L}^2 X_{Q_L}] - \sum_{\ell, Q} [Y_{\ell_R}^2 X_{\ell_R} + 3Y_{Q_R}^2 X_{Q_R}] \\
\text{U}(1)_Y [\text{U}(1)_X]^2 &\rightarrow A_Y = \sum_{\ell, Q} [Y_{\ell_L} X_{\ell_L}^2 + 3Y_{Q_L} X_{Q_L}^2] - \sum_{\ell, Q} [Y_{\ell_R} X_{\ell_R}^2 + 3Y_{Q_R} X_{Q_R}^2] \\
[\text{U}(1)_X]^3 &\rightarrow A_X = \sum_{\ell, Q} [X_{\ell_L}^3 + 3X_{Q_L}^3 - X_{\ell_R}^3 - 3X_{Q_R}^3] \\
[\text{Grav}]^2 \text{U}(1)_X &\rightarrow A_G = \sum_{\ell, Q} [X_{\ell_L} + 3X_{Q_L} - X_{\ell_R} - 3X_{Q_R}].
\end{aligned}$$

where the second equation counts only $SU(2)$ doublets, Q and ℓ runs over all quarks and leptons respectively and Y is the corresponding weak hypercharge. Moreover, electric charge definition given by the Gell-Mann-Nishijima relationship remains unaltered as $Q = \sigma_3/2 + Y/2$, where σ^a represents Pauli matrices while the new gauge symmetry adds a new term in the covariant derivative which now reads as:

$$D_\mu = \partial_\mu - \frac{ig}{2} W_\mu^\alpha \sigma_\alpha - ig' \frac{Y}{2} B_\mu - ig_X X Z'_\mu. \quad (3)$$

III. SCALAR BOSONS

First, the most general scalar potential allowed by symmetries is given by:

$$\begin{aligned}
V &= \mu_1^2 \phi_1^\dagger \phi_1 + \mu_2^2 \phi_2^\dagger \phi_2 + \mu_\chi^2 \chi^* \chi + \frac{f}{\sqrt{2}} (\phi_1^\dagger \phi_2 \chi^* + \text{H.C.}) \\
&+ \lambda_1 (\phi_1^\dagger \phi_1)^2 + \lambda_2 (\phi_2^\dagger \phi_2)^2 + \lambda_3 (\chi^* \chi)^2 \\
&+ \lambda_5 (\phi_1^\dagger \phi_1) (\phi_2^\dagger \phi_2) + \lambda'_5 (\phi_1^\dagger \phi_2) (\phi_2^\dagger \phi_1) \\
&+ \lambda_6 (\phi_1^\dagger \phi_1) (\chi^* \chi) + \lambda_7 (\phi_2^\dagger \phi_2) (\chi^* \chi).
\end{aligned} \quad (4)$$

This potential generates a mass matrix for charged, CP-even and CP-odd scalars after SSB takes place. For charged scalars, the mass matrix written in the basis (ϕ_1^\pm, ϕ_2^\pm) is:

$$M_C^2 = \frac{1}{4} \begin{pmatrix} -f \frac{v_\chi v_2}{v_1} - \lambda'_5 v_2^2 & f v_\chi + \lambda'_5 v_1 v_2 \\ f v_\chi + \lambda'_5 v_1 v_2 & -f \frac{v_\chi v_1}{v_2} - \lambda'_5 v_1^2 \end{pmatrix}, \quad (5)$$

whose rotation matrix connects interaction states to the mass eigenstates $\mathbf{H}^\pm = (G_W^\pm, H^\pm)$ given by:

$$\begin{aligned}
\phi^\pm &= \mathbb{R}_\phi \mathbf{H}^\pm, \\
\begin{pmatrix} \phi_1^\pm \\ \phi_2^\pm \end{pmatrix} &= \begin{pmatrix} c_\beta & s_\beta \\ -s_\beta & c_\beta \end{pmatrix} \begin{pmatrix} \mathbf{H}^\pm \\ G_W^\pm \end{pmatrix},
\end{aligned} \quad (6)$$

where $s_\beta = \sin \beta$, $c_\beta = \cos \beta$, $t_\beta = s_\beta/c_\beta = v_1/v_2$ with $v_1 > v_2$ and the corresponding mass eigenvalues are:

$$\begin{aligned}
m_{G_W^\pm}^2 &= 0, \\
m_{\mathbf{H}^\pm}^2 &= -\frac{1}{4} \frac{f v_\chi}{s_\beta c_\beta} - \frac{1}{4} \lambda'_5 v^2,
\end{aligned} \quad (7)$$

and G_W^\pm is identified as the would-be Goldstone boson eaten by the W gauge boson.

Regarding the neutral bosons, the CP-odd scalar bosons of the model $\boldsymbol{\eta} = (\eta_1, \eta_2, \zeta_\chi)$ mix them together according to the mass matrix:

$$M_I^2 = -\frac{f}{4} \begin{pmatrix} \frac{v_2 v_\chi}{v_1} & -v_\chi & v_2 \\ -v_\chi & \frac{v_1 v_\chi}{v_2} & -v_1 \\ v_2 & -v_1 & \frac{v_1 v_2}{v_\chi} \end{pmatrix}, \quad (8)$$

whose mass eigenstates $\mathbf{A} = (A^0, G_Z, G'_Z)$ contains only one physical pseudoscalar particle identified as A^0 , with mass given by:

$$m_{A^0}^2 = -\frac{1}{4} \frac{f v_\chi}{s_\beta c_\beta c_\gamma^2} \approx -\frac{1}{4} \frac{f v_\chi}{s_\beta c_\beta}, \quad (9)$$

where $t_\gamma = \tan \gamma = v s_\beta c_\beta / v_\chi \ll 1$ and, G_Z, G'_Z correspond to the massless Goldstone bosons eaten by the Z and Z' physical gauge bosons, respectively. The CP-even bosons mix together according to:

$$\begin{aligned} \boldsymbol{\eta} &= \mathbb{R}_\eta \mathbf{A}, \\ \begin{pmatrix} \eta_1 \\ \eta_2 \\ \zeta_\chi \end{pmatrix} &= \begin{pmatrix} c_\beta & s_\beta & 0 \\ -s_\beta & c_\beta & 0 \\ 0 & 0 & 1 \end{pmatrix} \begin{pmatrix} c_\gamma & 0 & -s_\gamma \\ 0 & 1 & 0 \\ s_\gamma & 0 & c_\gamma \end{pmatrix} \begin{pmatrix} A^0 \\ G_Z \\ G'_Z \end{pmatrix} \\ &= \begin{pmatrix} c_\beta c_\gamma & s_\beta & -c_\beta s_\gamma \\ -s_\beta c_\gamma & c_\beta & s_\beta s_\gamma \\ s_\gamma & 0 & c_\gamma \end{pmatrix} \begin{pmatrix} A^0 \\ G_Z \\ G'_Z \end{pmatrix}. \end{aligned} \quad (10)$$

Lastly, the CP-even scalar bosons of the model $\mathbf{h} = (h_1, h_2, \xi_\chi)$ give rise to the following mass matrix:

$$M_R^2 = \begin{pmatrix} \lambda_1 v_1^2 - \frac{1}{4} \frac{f v_\chi v_2}{v_1} & \hat{\lambda}_5 v_1 v_2 + \frac{1}{4} f v_\chi & \frac{1}{4} \lambda_6 v_1 v_\chi + \frac{1}{4} f v_2 \\ \hat{\lambda}_5 v_1 v_2 + \frac{1}{4} f v_\chi & \lambda_2 v_2^2 - \frac{1}{4} \frac{f v_\chi v_1}{v_2} & \frac{1}{4} \lambda_7 v_2 v_\chi + \frac{1}{4} f v_1 \\ \frac{1}{4} \lambda_6 v_1 v_\chi + \frac{1}{4} f v_2 & \frac{1}{4} \lambda_7 v_2 v_\chi + \frac{1}{4} f v_1 & \lambda_3 v_\chi^2 - \frac{1}{4} \frac{f v_1 v_2}{v_\chi} \end{pmatrix},$$

that provide the mass eigenstates $\mathbf{H} = (H, h, H_\chi)$ with masses:

$$m_h^2 \approx \left(\tilde{\lambda}_1 c_\beta^4 + 2 \tilde{\lambda}_5 c_\beta^2 s_\beta^2 + \tilde{\lambda}_2 s_\beta^4 \right) v^2, \quad (11)$$

$$m_H^2 \approx -\frac{f v_\chi}{4 s_\beta c_\beta}, \quad (12)$$

$$m_{H_\chi}^2 \approx \lambda_3 v_\chi^2. \quad (13)$$

where the tilded constants are defined as:

$$\tilde{\lambda}_1 = \lambda_1 - \frac{\lambda_6^2}{4 \lambda_3} - \frac{\lambda_7^2}{4 \lambda_3 t_\beta^2}, \quad (14)$$

$$\tilde{\lambda}_2 = \lambda_2 - \frac{\lambda_6^2 t_\beta^2}{4 \lambda_3} - \frac{\lambda_7^2}{4 \lambda_3}, \quad (15)$$

$$\tilde{\lambda}_5 = \hat{\lambda}_5 - \frac{\lambda_6^2 t_\beta}{2 \lambda_3} - \frac{\lambda_7^2}{2 \lambda_3 t_\beta}, \quad (16)$$

and the rotation matrix written as the product of three matrices is given by:

$$\begin{pmatrix} h_1 \\ h_2 \\ \xi_\chi \end{pmatrix} = \begin{pmatrix} 1 & 0 & 0 \\ 0 & c_{23} & s_{23} \\ 0 & -s_{23} & c_{23} \end{pmatrix} \begin{pmatrix} c_{13} & 0 & s_{13} \\ 0 & 1 & 0 \\ -s_{13} & 0 & c_{13} \end{pmatrix} \begin{pmatrix} c_\alpha & s_\alpha & 0 \\ -s_\alpha & c_\alpha & 0 \\ 0 & 0 & 1 \end{pmatrix} \begin{pmatrix} H \\ h \\ H_\chi \end{pmatrix}, \quad (17)$$

where the mixing angles are given by

$$s_{23} = \frac{\lambda_7 c_\beta v}{2\lambda_3 v_\chi}, \quad s_{13} = \frac{\lambda_6 s_\beta v}{2\lambda_3 v_\chi}, \quad t_{2\alpha} = \frac{f v_\chi + 2\tilde{\lambda}_5 s_\beta c_\beta v^2}{f v_\chi + 2t_{2\beta}(\tilde{\lambda}_1 s_\beta^2 - \tilde{\lambda}_2 c_\beta^2)v^2} t_{2\beta}. \quad (18)$$

As it will be shown in section VI, the top quark mass is proportional to v_1 while the down quark is proportional to v_2 , so their mass difference can be understood by the value of each VEV. Thus, it is appropriate to consider some approximations that can be done assuming $s_\beta \approx 1$:

$$c_\beta \approx 0, \quad t_\alpha \approx t_\beta, \quad s_{13} \approx \frac{\lambda_6 v s_\beta}{2\lambda_3 v_\chi}, \quad s_{23} \approx 0, \quad (19)$$

which reduces the mixing matrix for the CP-even as:

$$\begin{aligned} \mathbf{h} &= \mathbb{R}_h \mathbf{H}, \\ \begin{pmatrix} h_1 \\ h_2 \\ \xi_\chi \end{pmatrix} &= \begin{pmatrix} c_{13} & 0 & s_{13} \\ 0 & 1 & 0 \\ -s_{13} & 0 & c_{13} \end{pmatrix} \begin{pmatrix} c_\alpha & s_\alpha & 0 \\ -s_\alpha & c_\alpha & 0 \\ 0 & 0 & 1 \end{pmatrix} \begin{pmatrix} H \\ h \\ H_\chi \end{pmatrix} \\ &= \begin{pmatrix} c_\beta c_{13} & s_\beta c_{13} & s_{13} \\ -s_\beta & c_\beta & 0 \\ -c_\beta s_{13} & s_\beta s_{13} & c_{13} \end{pmatrix} \begin{pmatrix} H \\ h \\ H_\chi \end{pmatrix}. \end{aligned} \quad (20)$$

From the three CP-even physical states, the lightest one, h , is identified as the SM Higgs boson, while H and H_χ are heavier and yet unobserved particles whose mass depends on the $U(1)_X$ symmetry breaking scale v_χ similarly to A^0 and \mathbf{H}^\pm are. Therefore, heavy scalars have approximately the same mass, $m_H \approx m_{H_\chi} \approx m_{A^0} \approx m_{\mathbf{H}^\pm}$ and according to the lower bound on charged scalar given by [2] we can assume a lower bound for their masses around 800 GeV.

IV. GAUGE BOSONS

After SSB, the charged gauge bosons $W_\mu^\pm = (W_\mu^1 \mp W_\mu^2)/\sqrt{2}$ acquire a mass given by $m_W = gv/2$ yielding the restriction $\sqrt{v_1^2 + v_2^2} = 246.22$ GeV. Regarding the neutral gauge bosons of the model, they are arranged in the basis (W_μ^3, B_μ, Z'_μ) , producing the following mass matrix:

$$M_0^2 = \frac{1}{4} \begin{pmatrix} g^2 v^2 & -gg'v^2 & -\frac{2}{3}gg_X v^2(1+c_\beta^2) \\ * & g'^2 v^2 & \frac{2}{3}g'g_X v^2(1+c_\beta^2) \\ * & * & \frac{4}{9}g_X^2 v_\chi^2 \left[1 + (1+3c_\beta^2)\frac{v^2}{v_\chi^2}\right] \end{pmatrix},$$

and their states mix them together in order to get the mass eigenstates $(A_\mu, Z_\mu^1, Z_\mu^2)$:

$$\begin{pmatrix} W_\mu^3 \\ B_\mu \\ Z'_\mu \end{pmatrix} = \begin{pmatrix} s_W & c_W & 0 \\ c_W & -s_W & 0 \\ 0 & 0 & 1 \end{pmatrix} \begin{pmatrix} 1 & 0 & 0 \\ 0 & c_Z & -s_Z \\ 0 & s_Z & c_Z \end{pmatrix} \begin{pmatrix} A_\mu \\ Z_\mu^1 \\ Z_\mu^2 \end{pmatrix}, \quad (21)$$

where the Weinberg angle is defined as $t_W = s_W/c_W = \tan \theta_W = g'/g$ and $\sin \theta_Z = s_Z$:

$$s_Z \approx (1 + s_\beta^2) \frac{2g_X c_W}{3g} \frac{M_Z}{M_{Z'}} \approx \frac{2v}{v_\chi} \lesssim 10^{-2}, \quad (22)$$

where in the last approximation we have assumed $t_\beta \gg 1$ and θ_Z as a small mixing angle between Z and Z' gauge boson since they are not truly mass eigenstates. Then, the masses for the neutral gauge bosons are given by:

$$M_1 \approx M_Z = \frac{gv}{2c_W}, \quad M_2 \approx M_{Z'} \approx \frac{g_X v_\chi}{3}. \quad (23)$$

Recent bounds on Z' searches sets a lower bound of $M_{Z'} > 4.1$ TeV for the Sequential Standard Model [27], which according to Eq. (23) results in a lower bound for v_χ of $v_\chi > 15$ TeV if $g_X \sim g$. Nevertheless, the prediction of the model on the Z' mass is above 6 TeV from the $pp \rightarrow \ell^+ \ell^-$ process [28] at 3σ . However, the smallness of s_Z allows to approximate $c_Z \approx 1$, yielding them the total mixing of the neutral gauge bosons, which can be written as:

$$\begin{pmatrix} W_\mu^3 \\ B_\mu \\ Z'_\mu \end{pmatrix} \approx \begin{pmatrix} s_W & c_W c_Z & -c_W s_Z \\ c_W & -s_W c_Z & s_W s_Z \\ 0 & s_Z & c_Z \end{pmatrix} \begin{pmatrix} A_\mu \\ Z_\mu^1 \\ Z_\mu^2 \end{pmatrix}. \quad (24)$$

V. CHARGED LEPTON MASSES

The most general interaction Lagrangian involving charged leptons according to the $U(1)_X \otimes \mathbb{Z}_2$ symmetry is given by:

$$-\mathcal{L}_\ell = \eta \bar{\ell}_L^e \phi_2 e_R^\mu + h \bar{\ell}_L^\mu \phi_2 e_R^\mu + \zeta \bar{\ell}_L^\tau \phi_2 e_R^e + H \bar{\ell}_L^\tau \phi_2 e_R^\tau + q_{11} \bar{\ell}_L^e \phi_1 E_R + q_{21} \bar{\ell}_L^\mu \phi_1 E_R + g_{\chi E} \bar{E}_L \chi E_R + g_{\chi \mathcal{E}} \bar{\mathcal{E}}_L \chi^* \mathcal{E}_R + \text{H.C.} \quad (25)$$

The \mathcal{E} lepton is decoupled and gets mass $m_\mathcal{E} = g_{\chi \mathcal{E}} v_\chi / \sqrt{2}$ while after SSB the Lagrangian gives rise to a 4×4 mass matrix spanned in the flavor basis $\mathbf{E} = (e^e, e^\mu, e^\tau, E)$ which can be written as:

$$\mathbb{M}_E^0 = \left(\begin{array}{ccc|c} 0 & \frac{\eta v_2}{\sqrt{2}} & 0 & \frac{q_{11} v_1}{\sqrt{2}} \\ 0 & \frac{h v_2}{\sqrt{2}} & 0 & \frac{q_{12} v_1}{\sqrt{2}} \\ \frac{\zeta v_2}{\sqrt{2}} & 0 & \frac{H v_2}{\sqrt{2}} & 0 \\ 0 & 0 & 0 & \frac{g_{\chi E} v_\chi}{\sqrt{2}} \end{array} \right). \quad (26)$$

Such a matrix has rank 3, which means that the lightest lepton, the electron, is massless at tree-level. In this point, we consider the following effective operators up to dimension 7, invariant under the symmetry of the model, to explain the electron mass:

$$\begin{aligned} \mathcal{O}_{ij}^\ell &= \Omega_{ij}^\ell \left(\frac{\chi^*}{\Lambda} \right)^3 \bar{\ell}_L^i \phi_2 e_R^j, & \mathcal{O}_{\tau\mu}^\ell &= \Omega_{32}^\ell \left(\frac{\chi}{\Lambda} \right)^3 \bar{\ell}_L^\tau \phi_2 e_R^\mu, \\ \mathcal{O}_{Ej}^\ell &= \frac{\Omega_{4j}^\ell}{\Lambda} (\phi_2^\dagger \phi_1) \bar{E}_L e_R^j, & \mathcal{O}_{E\mu}^\ell &= \frac{\Omega_{42}^\ell}{\Lambda^2} (\phi_1^\dagger \phi_2) \chi \bar{E}_L e_R^\mu, \\ \mathcal{O}_{\tau E}^\ell &= \Omega_{34}^\ell \left(\frac{\chi}{\Lambda} \right)^3 \hat{\ell}_L^\tau \phi_1 E_R, \end{aligned} \quad (27)$$

where $i = e, \mu$, $j = e, \tau$ and Λ is the associated energy scale. Then, the new mass matrix reads:

$$\mathbb{M}_E = \left(\begin{array}{ccc|c} \Omega_{11}^\ell \frac{v_2 v_\chi^3}{4\Lambda^3} & \frac{\eta v_2}{\sqrt{2}} & \Omega_{13}^\ell \frac{v_2 v_\chi^3}{4\Lambda^3} & \frac{q_{11} v_1}{\sqrt{2}} \\ \Omega_{21}^\ell \frac{v_2 v_\chi^3}{4\Lambda^3} & \frac{h v_2}{\sqrt{2}} & \Omega_{23}^\ell \frac{v_2 v_\chi^3}{4\Lambda^3} & \frac{q_{12} v_1}{\sqrt{2}} \\ \frac{\zeta v_2}{\sqrt{2}} & \Omega_{32}^\ell \frac{v_2 v_\chi^3}{4\Lambda^3} & \frac{H v_2}{\sqrt{2}} & \Omega_{34}^\ell \frac{v_1 v_\chi^3}{4\Lambda^3} \\ \frac{v_1 v_2}{2\Lambda} \Omega_{41}^\ell & \frac{v_1 v_2 v_\chi}{2\sqrt{2}\Lambda^2} \Omega_{42}^\ell & \frac{v_1 v_2}{2\Lambda} \Omega_{43}^\ell & \frac{g_{\chi E} v_\chi}{\sqrt{2}} \end{array} \right). \quad (28)$$

The diagonalization matrix for left(right)-handed leptons $\mathbb{V}_{L(R)}^E$ to get the mass eigenstates $\mathbf{e} = (e, \mu, \tau, E)$ is then given by

$$\mathbf{E}_L = \mathbb{V}_L^E \mathbf{e}_L, \quad \mathbf{E}_R = \mathbb{V}_R^E \mathbf{e}_R, \quad (29)$$

and the rotation matrices can be approximated to $\mathbb{V}_L^E \approx \mathbb{V}_{L1}^E \mathbb{V}_{L2}^E$ and $\mathbb{V}_R^E \approx \mathbb{V}_{R1}^E \mathbb{V}_{R2}^E$ being each matrix defined as:

$$\begin{aligned} \mathbb{V}_{L1}^E &\approx \begin{pmatrix} 1 & 0 & 0 & \frac{v_1 q_{11}}{\sqrt{2}m_E} \\ 0 & 1 & 0 & \frac{v_1 q_{12}}{\sqrt{2}m_E} \\ 0 & 0 & 1 & r_3 \\ -\frac{v_1 q_{11}}{\sqrt{2}m_E} & -\frac{v_1 q_{12}}{\sqrt{2}m_E} & -r_3 & 1 \end{pmatrix}, & \mathbb{V}_{L2}^E &\approx \begin{pmatrix} c_{e\mu} & s_{e\mu} & r_1 & 0 \\ -s_{e\mu} & c_{e\mu} & r_2 & 0 \\ -r_1 c_{e\mu} + r_2 s_{e\mu} & -r_2 c_{e\mu} - r_1 s_{e\mu} & 1 & 0 \\ 0 & 0 & 0 & 1 \end{pmatrix}, \\ \mathbb{V}_{R1}^E &\approx \begin{pmatrix} 1 & 0 & 0 & \frac{\Omega_{41}^\ell v_1 v_2}{2m_E \Lambda^2} \\ 0 & 1 & 0 & t_1 \\ 0 & 0 & 1 & \frac{\Omega_{43}^\ell v_1 v_2}{2m_E \Lambda^2} \\ -\frac{\Omega_{41}^\ell v_1 v_2}{2m_E \Lambda^2} & -t_1 & -\frac{\Omega_{43}^\ell v_1 v_2}{2m_E \Lambda^2} & 1 \end{pmatrix}, & \mathbb{V}_{R2}^E &\approx \begin{pmatrix} c_{e\tau} & -c_{e\tau} t_2 & s_{e\tau} & 0 \\ t_2 & 1 & 0 & 0 \\ -s_{e\tau} & -s_{e\tau} t_2 & c_{e\tau} & 0 \\ 0 & 0 & 0 & 1 \end{pmatrix}, \end{aligned} \quad (30)$$

where

$$\begin{aligned} r_1 &= \frac{(s_{e\tau} \Omega_{11}^\ell + c_{e\tau} \Omega_{13}^\ell) v_2 v_\chi^3 + \sqrt{2} m_\mu v_\chi^3 \Omega_{32}^\ell s_{e\mu}}{4\Lambda^3 m_\tau}, & r_2 &= \frac{(s_{e\tau} \Omega_{21}^\ell + c_{e\tau} \Omega_{23}^\ell) v_2 v_\chi^3 + \sqrt{2} m_\mu v_\chi^3 \Omega_{32}^\ell s_{e\mu}}{4\Lambda^3 m_\tau}, \\ r_3 &= \frac{v_1 v_2}{2\Lambda m_E} \left(\frac{\Omega_{34}^\ell v_\chi^3}{2\Lambda^2 v_2} + \frac{m_\tau (\Omega_{41}^\ell s_{e\tau} - \Omega_{43}^\ell c_{e\tau})}{m_E} \right), & t_1 &= \frac{\Omega_{42}^\ell v_1 v_2 v_\chi}{2m_E \Lambda^2} + \frac{v_1 m_\mu}{\sqrt{2} m_E^2} (q_{11} s_{e\mu} + q_{12} c_{e\mu}), \\ t_2 &= \frac{v_2 v_\chi^3}{4\Lambda^3 m_\mu} (s_{e\mu} (\Omega_{13}^\ell s_{e\tau} - \Omega_{11}^\ell c_{e\tau}) + c_{e\mu} (\Omega_{21}^\ell c_{e\tau} + \Omega_{23}^\ell s_{e\tau})), \end{aligned} \quad (31)$$

with $t_{e\mu} = \eta/h$ and $t_{e\tau} = \zeta/H$. Lastly, the mass eigenvalues are given by:

$$m_e^2 \approx \frac{v_1^4 v_2^2}{4} \left(\frac{s_{e\tau} v_\chi^3 (\Omega_{23}^\ell s_{e\mu} - \Omega_{13}^\ell c_{e\mu})}{v_1^2 \Lambda^3} + \frac{c_{e\tau} v_\chi^3 (\Omega_{11}^\ell c_{e\mu} - \Omega_{21}^\ell s_{e\mu})}{v_1^2 \Lambda^3} + \frac{(q_{11} c_{e\mu} - q_{12} s_{e\mu}) (\Omega_{43}^\ell s_{e\tau} - \Omega_{41}^\ell c_{e\tau})}{\sqrt{2} m_E \Lambda} \right)^2, \quad (32)$$

$$m_\mu^2 \approx \frac{1}{2} (\eta^2 + h^2) v_2^2, \quad (33)$$

$$m_\tau^2 \approx \frac{1}{2} (\zeta^2 + H^2) v_2^2, \quad (34)$$

$$m_E^2 \approx \frac{1}{2} g_{\chi E}^2 v_\chi^2. \quad (35)$$

Mass eigenvalues impose some restrictions on the parameter space we have considered, $\{\eta, \zeta, g_{\chi E}, q_{11}, q_{12}, \Omega_{ij}\}$. In particular, the mass of the top quark depends on v_1 while the bottom quark and the τ lepton depends on v_2 , so we can assume that such masses can be understood by the VEVs values and Yukawa couplings of order 1. Thus, we choose $v_1 = 246$ GeV and $v_2 \approx 1$ GeV. Moreover, electron mass provides the energy scale Λ , so, by giving a random value between 1 and 10 to all free parameters, we can find the allowed region for Λ as a function of v_χ as shown in figure 1. It can be seen that there is an upper bound of $\Lambda \leq \sqrt[3]{9.4 \frac{v_2}{4m_e}} v_\chi \approx 17 v_\chi$.

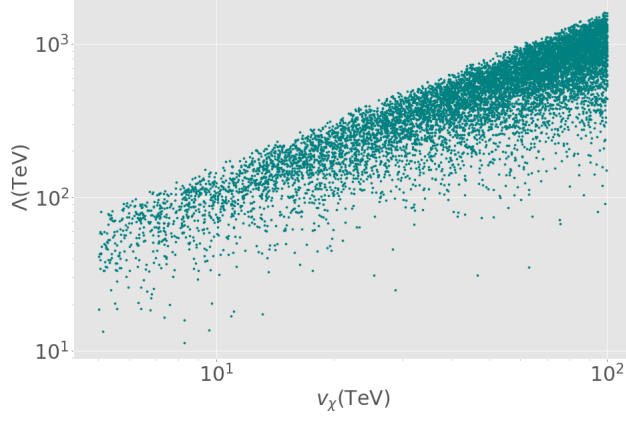


FIG. 1: Monte Carlo exploration for Λ as a function of v_χ according to the electron mass by exploring the parameter space of Eq.(32).

VI. QUARK MIXING

Since the new symmetry has a non-universal X charge assignation, Z_2^μ flavor-changing neutral current interactions are present in the Lagrangian. Then, prior to considering the relevant interaction Lagrangian for the $b \rightarrow s \ell^+ \ell^-$ transition, we need to consider the rotation matrix that connects flavor and mass eigenstates for the quark sector. The most general Yukawa Lagrangian allowed by gauge symmetry is given by:

$$\begin{aligned} -\mathcal{L}_U &= \bar{q}_L^1 (\tilde{\phi}_2 h_2^U)_{12} U_R^2 + \bar{q}_L^2 (\tilde{\phi}_1 h_1^U)_{22} U_R^2 + \bar{q}_L^3 (\tilde{\phi}_1 h_1^U)_{31} U_R^1 + \bar{q}_L^3 (\tilde{\phi}_1 h_1^U)_{33} U_R^3 \\ &\quad + \bar{T}_L (\chi h_\chi^U)_2 U_R^2 + \bar{T}_L (\chi h_\chi^T) T_R + \bar{q}_L^1 (\tilde{\phi}_2 h_2^T)_1 T_R + \bar{q}_L^2 (\tilde{\phi}_1 h_1^T)_2 T_R \\ -\mathcal{L}_D &= \bar{q}_L^3 (\phi_2 h_2^D)_{3j} D_R^j + \bar{q}_L^1 (\phi_1 h_1^J)_m J_R^m + \bar{q}_L^2 (\phi_2 h_2^J)_m J_R^m + \bar{J}_L^p (\chi^* h_\chi^J)_{nm} J_R^m + \text{H.C.}, \end{aligned}$$

where $\tilde{\phi}_{1,2} = i\sigma_2 \phi_{1,2}^*$ are conjugate fields, $j = 1, 2, 3$ label the right-handed fermions and $n(m) = 1, 2$ is the index of the exotic $\mathcal{J}^{n(m)}$ quarks. After SSB takes place, such Lagrangians give rise to the following mass matrices:

$$\mathbb{M}_U^0 = \left(\begin{array}{ccc|c} 0 & \frac{(h_2^U)_{12} v_2}{\sqrt{2}} & 0 & \frac{(h_2^T)_{12} v_2}{\sqrt{2}} \\ 0 & \frac{(h_1^U)_{22} v_1}{\sqrt{2}} & 0 & \frac{(h_1^T)_{22} v_1}{\sqrt{2}} \\ \frac{(h_1^U)_{13} v_1}{\sqrt{2}} & 0 & \frac{(h_1^U)_{33} v_1}{\sqrt{2}} & 0 \\ 0 & \frac{(h_\chi^U)_{22} v_\chi}{\sqrt{2}} & 0 & \frac{h_\chi^T v_\chi}{\sqrt{2}} \end{array} \right), \quad \mathbb{M}_D^0 = \left(\begin{array}{ccc|c|c} 0 & 0 & 0 & \frac{v_1 (h_1^J)_{11}}{\sqrt{2}} & \frac{v_1 (h_1^J)_{12}}{\sqrt{2}} \\ 0 & 0 & 0 & \frac{v_2 (h_2^J)_{11}}{\sqrt{2}} & \frac{v_2 (h_2^J)_{12}}{\sqrt{2}} \\ \frac{v_2 (h_2^D)_{31}}{\sqrt{2}} & \frac{v_2 (h_2^D)_{32}}{\sqrt{2}} & \frac{v_2 (h_2^D)_{33}}{\sqrt{2}} & 0 & 0 \\ 0 & 0 & 0 & \frac{v_\chi (h_\chi^J)_{11}}{\sqrt{2}} & \frac{v_\chi (h_\chi^J)_{12}}{\sqrt{2}} \\ 0 & 0 & 0 & \frac{v_\chi (h_\chi^J)_{21}}{\sqrt{2}} & \frac{v_\chi (h_\chi^J)_{22}}{\sqrt{2}} \end{array} \right). \quad (36)$$

A. Up quarks

In the case of up-like quarks, the mass matrix has rank 3 which means that the up quark is massless. Similarly to the electron, we can consider the following set of dimension 5 effective operators:

$$\begin{aligned} \mathcal{O}_{11}^U &= \Omega_{11}^U \frac{\chi^*}{\Lambda} \bar{q}_L^1 \tilde{\phi}_1 U_R^1, & \mathcal{O}_{13}^U &= \Omega_{13}^U \frac{\chi^*}{\Lambda} \bar{q}_L^1 \tilde{\phi}_1 U_R^3, \\ \mathcal{O}_{21}^U &= \Omega_{21}^U \frac{\chi}{\Lambda} \bar{q}_L^2 \tilde{\phi}_2 U_R^1, & \mathcal{O}_{23}^U &= \Omega_{23}^U \frac{\chi}{\Lambda} \bar{q}_L^2 \tilde{\phi}_2 U_R^3, \\ \mathcal{O}_{32}^U &= \Omega_{32}^U \frac{\chi}{\Lambda} \bar{q}_L^3 \tilde{\phi}_2 U_R^2, & \mathcal{O}_{34}^U &= \Omega_{34}^U \frac{\chi}{\Lambda} \bar{q}_L^3 \tilde{\phi}_2 \mathcal{T}_R, \\ \mathcal{O}_{41}^U &= \Omega_{41}^U \frac{\phi_1^\dagger \phi_2}{\Lambda} \bar{\mathcal{T}}_L U_R^1, & \mathcal{O}_{43}^U &= \Omega_{43}^U \frac{\phi_1^\dagger \phi_2}{\Lambda} \bar{\mathcal{T}}_L U_R^3, \end{aligned}$$

so all zeros in the mass matrix are filled, yielding the following new mass matrix:

$$\mathbb{M}_U = \left(\begin{array}{ccc|c} \Omega_{11}^U v_1 \frac{v_\chi}{2\Lambda} & \frac{(h_2^U)_{12} v_2}{\sqrt{2}} & \Omega_{13}^U v_1 \frac{v_\chi}{2\Lambda} & \frac{(h_2^T)_{12} v_2}{\sqrt{2}} \\ \Omega_{21}^U v_2 \frac{v_\chi}{2\Lambda} & \frac{(h_1^U)_{22} v_1}{\sqrt{2}} & \Omega_{23}^U v_2 \frac{v_\chi}{2\Lambda} & \frac{(h_1^T)_{22} v_1}{\sqrt{2}} \\ \frac{(h_1^U)_{13} v_1}{\sqrt{2}} & \Omega_{32}^U v_2 \frac{v_\chi}{2\Lambda} & \frac{(h_1^U)_{33} v_1}{\sqrt{2}} & \Omega_{34}^U v_2 \frac{v_\chi}{2\Lambda} \\ \hline \Omega_{41}^U v_1 \frac{v_2}{2\Lambda} & \frac{(h_\chi^U)_{22} v_\chi}{\sqrt{2}} & \Omega_{43}^U v_1 \frac{v_2}{2\Lambda} & \frac{h_\chi^T v_\chi}{\sqrt{2}} \end{array} \right). \quad (37)$$

In order to provide mass eigenvalues and rotation matrices, we introduce the following set of rotated parameters:

$$\begin{aligned} \begin{pmatrix} r_1^+ \\ r_1^- \end{pmatrix} &= \begin{pmatrix} \cos \alpha & -\sin \alpha \\ \sin \alpha & \cos \alpha \end{pmatrix} \begin{pmatrix} (h_2^T)_1 \\ (h_2^U)_{12} \end{pmatrix}, & \begin{pmatrix} r_2^+ \\ r_2^- \end{pmatrix} &= \begin{pmatrix} \cos \alpha & -\sin \alpha \\ \sin \alpha & \cos \alpha \end{pmatrix} \begin{pmatrix} (h_1^T)_2 \\ (h_1^U)_{22} \end{pmatrix}, \\ \begin{pmatrix} r_3^+ \\ r_3^- \end{pmatrix} &= \begin{pmatrix} \cos \alpha & -\sin \alpha \\ \sin \alpha & \cos \alpha \end{pmatrix} \begin{pmatrix} \Omega_{34}^U \\ \Omega_{32}^U \end{pmatrix}, & \tan \alpha &= \frac{h_\chi^T}{(h_\chi^U)_2}, \end{aligned} \quad (38)$$

Then, we can write the mass eigenvalues as:

$$m_u^2 \approx \frac{v_\chi^2}{4\Lambda^2} \left(v_1 s_{uc} (\Omega_{13}^U s_{ut} - \Omega_{11}^U c_{ut}) + v_2 c_{uc} (-\Omega_{23}^U s_{ut} + \Omega_{21}^U c_{ut}) \right)^2, \quad (39)$$

$$m_c^2 \approx \frac{1}{2} (v_2^2 r_1^{+2} + v_1^2 r_2^{+2}), \quad (40)$$

$$m_t^2 \approx \frac{1}{2} v_1^2 [(h_1^U)_{13}]^2 + [(h_1^U)_{33}]^2, \quad (41)$$

$$m_T^2 \approx \frac{1}{2} v_\chi^2 [(h_\chi^T)^2 + ((h_\chi^U)_2)^2]. \quad (42)$$

where

$$\tan \theta_{uc} = t_{uc} = \frac{v_2 r_1^+}{v_1 r_2^-} = \frac{v_2 (h_2^T)_1 (h_\chi^U)_2 - (h_2^U)_{12} h_\chi^T}{v_1 (h_1^T)_2 (h_\chi^U)_2 - (h_1^U)_{22} h_\chi^T}, \quad \tan \theta_{ut} = \frac{(h_1^U)_{13}}{(h_1^U)_{33}}. \quad (43)$$

In a similar fashion to the charged leptons, left-handed quark rotation matrix can be written as $\mathbb{V}_L^U \approx \mathbb{V}_{L1}^U \mathbb{V}_{L2}^U$ while for right-handed quarks we have a single matrix \mathbb{V}_R^U . The explicit expression of the matrices are:

$$\begin{aligned} \mathbb{V}_{L1}^U &\approx \begin{pmatrix} 1 & 0 & 0 & \frac{v_2 r_1^-}{\sqrt{2} m_\tau} \\ 0 & 1 & 0 & \frac{v_1 r_2^-}{\sqrt{2} m_\tau} \\ 0 & 0 & 1 & \frac{v_2 v_\chi r_3^-}{2 m_\tau \Lambda} \\ -\frac{v_2 r_1^-}{\sqrt{2} m_\tau} & -\frac{v_1 r_2^-}{\sqrt{2} m_\tau} & -\frac{v_2 v_\chi r_3^-}{2 m_\tau \Lambda} & 1 \end{pmatrix}, & \mathbb{V}_{L2}^U &\approx \begin{pmatrix} c_{uc} & s_{uc} & r_1^U & 0 \\ -s_{uc} & c_{uc} & r_2^U & 0 \\ -r_1^U c_{uc} + r_2^U s_{uc} & -r_2^U c_{uc} - r_1^U s_{uc} & 1 & 0 \\ 0 & 0 & 0 & 1 \end{pmatrix}, \\ \mathbb{V}_R^U &\approx \begin{pmatrix} c_{ut} & 0 & s_{ut} & 0 \\ 0 & -s_\alpha & 0 & c_\alpha \\ -s_{ut} & 0 & c_{ut} & 0 \\ 0 & c_\alpha & 0 & s_\alpha \end{pmatrix}, \end{aligned} \quad (44)$$

where the r_1^U and r_2^U parameters are defined as:

$$r_1^U = \frac{v_\chi v_2^2 r_3^+ r_1^+}{2\sqrt{2} m_t^2 \Lambda} + \frac{v_\chi v_1 (\Omega_{11}^U s_{ut} + \Omega_{13}^U c_{ut})}{2 m_t \Lambda}, \quad r_2^U = \frac{v_1 v_2 v_\chi (\Omega_{21}^U s_{ut} + \Omega_{23}^U c_{ut} + r_3^+ r_2^+)}{2\sqrt{2} m_t^2 \Lambda}. \quad (45)$$

The mass matrix for the up quarks has a similar structure as charged leptons. We obtained that both muon and tau lepton are proportional to v_2 , where the quotient $m_\mu/m_\tau = 0.059$ can be understood with Yukawa couplings of order 1. Although, in the case of up quarks, having $m_c, m_t \propto v_1$ is not suitable due to the big mass difference between top and charm quarks. The mass matrix entry $(\mathbb{M}_U)_{42} = (h_\chi^U)_{22} v_\chi / \sqrt{2}$ makes the difference between up-quarks and

charged leptons. This entry together with the $(\mathbb{M}_U)_{24}$ entry contributes to the SM quark mixing through a seesaw mechanism between c and \mathcal{T} quarks, producing a Yukawa difference, as shown in the charm mass expression in Eq. (40), we can approximate it to:

$$m_c^2 \approx \frac{1}{2} v_1^2 r_2^{+2} \quad (46)$$

$$= \frac{1}{2} v_1^2 \frac{((h_1^T)_2 (h_\chi^U)_2 - (h_1^U)_{22} h_\chi^T)^2}{(h_\chi^U)_2^2 + (h_\chi^T)^2}. \quad (47)$$

Since all Yukawa couplings are of order 1, it would give a mass to the charm quark proportional to the top quark, but a suppression factor $(h_1^T)_2 c_\alpha - (h_1^U)_{22} s_\alpha$ resets the order of magnitude to 10^{-2} , consistent with the observed phenomenology:

$$\frac{m_c}{m_t} \approx \frac{(h_1^T)_2 c_\alpha - (h_1^U)_{22} s_\alpha}{\sqrt{((h_1^U)_{13})^2 + ((h_1^U)_{33})^2}} \sim 10^{-2}. \quad (48)$$

As a benchmark scenario, let us consider the particular case where $(h_1^U)_{13} = (h_1^U)_{33} = 1/\sqrt{2}$, and by considering $m_c = 1.280 \pm 0.025$ GeV[29] and $m_t = 172.69 \pm 0.48$ GeV[30], the ratio of masses becomes:

$$(7.33 \pm 0.124) \times 10^{-3} \approx (h_1^T)_2 c_\alpha - (h_1^U)_{22} s_\alpha. \quad (49)$$

This requirement can be easily achieved as it can be seen in figure 2, where we show the parameter region compatible with such a restriction for different values of α .

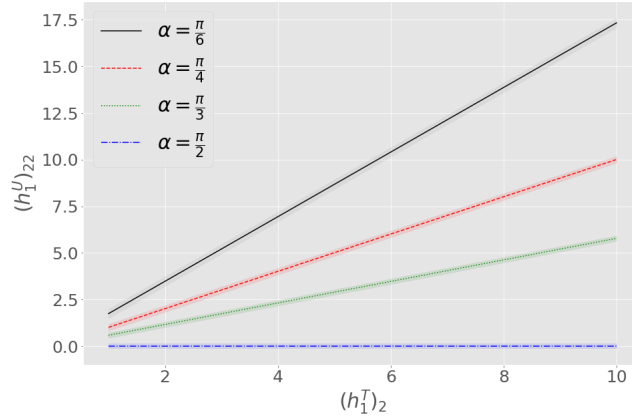


FIG. 2: Parameter region compatible with the charm and top masses.

We can also get an estimate of the higher dimensional operators energy scale from the up-quark mass. The Monte-carlo exploration gave uniformly distributed random values to the parameter space in Eq. (39) prior to numerically solve the equation for Λ . It shows that there is also an upper limit of $\Lambda \leq \frac{5v_1}{m_\nu} v_\chi \approx 5.6 \times 10^5 v_\chi$ as it can be seen in figure 3. Such an upper limit is several order of magnitude greater than the obtained from the electron mass despite they both have similar masses. It can be understood by noticing that effective operators that provide the electron mass are of dimension seven while effective operators responsible of the up-quark mass are of dimension five, requiring in the latter greater values of Λ to compensate the lack of exponentiation.

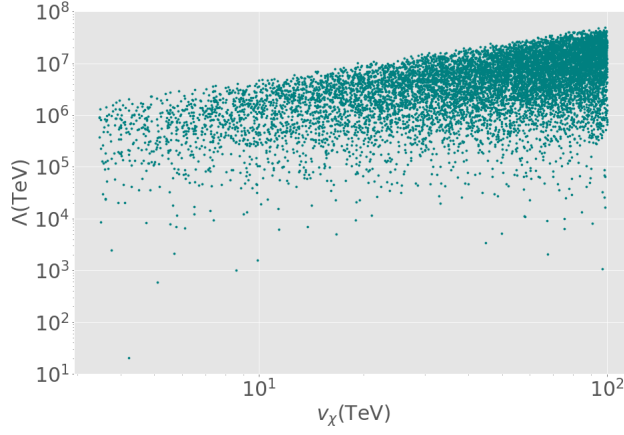


FIG. 3: Monte Carlo exploration for Λ as a function of ν_χ according to the up quark mass in Eq. (39).

B. Down quarks

Likewise, the down quark mass matrix written in the basis $\{d_1, d_2, d_3, \mathcal{J}^2, \mathcal{J}^2\}$, as shown in Eq. (36), has rank 3. In this case, there two lightest particles, identified as the down and strange quark, are massless. Then, we consider the following set of dimension 5 effective operators:

$$\mathcal{O}_{1j}^D = \Omega_{1j}^D \frac{\chi^*}{\Lambda} \bar{q}_L^1 \phi_2 D_R^j, \quad \mathcal{O}_{2j}^D = \Omega_{2j}^D \frac{\chi}{\Lambda} \bar{q}_L^2 \phi_1 D_R^j, \quad (50)$$

$$\mathcal{O}_{4j}^D = \Omega_{4j}^D \frac{\phi_2^\dagger \phi_1}{\Lambda} \bar{\mathcal{J}}_L^1 D_R^j, \quad \mathcal{O}_{5j}^D = \Omega_{5j}^D \frac{\phi_2^\dagger \phi_1}{\Lambda} \bar{\mathcal{J}}_L^2 D_R^j, \quad (51)$$

$$\mathcal{O}_{34}^D = \Omega_{34}^D \frac{\chi}{\Lambda} \bar{q}_L^3 \phi_2 \mathcal{J}_R^1, \quad \mathcal{O}_{35}^D = \Omega_{35}^D \frac{\chi}{\Lambda} \bar{q}_L^3 \phi_2 \mathcal{J}_R^2, \quad (52)$$

so all zeros are filled so the mass matrix now reads:

$$\mathbb{M}_D = \begin{pmatrix} \Omega_{11}^D v_2 \frac{v_\chi}{2\Lambda} & \Omega_{12}^D v_2 \frac{v_\chi}{2\Lambda} & \Omega_{13}^D v_2 \frac{v_\chi}{2\Lambda} & \frac{v_1(h_1^J)_1}{\sqrt{2}} & \frac{v_1(h_1^J)_2}{\sqrt{2}} \\ \Omega_{21}^D v_1 \frac{v_\chi}{2\Lambda} & \Omega_{22}^D v_1 \frac{v_\chi}{2\Lambda} & \Omega_{23}^D v_1 \frac{v_\chi}{2\Lambda} & \frac{v_2(h_2^J)_1}{\sqrt{2}} & \frac{v_2(h_2^J)_2}{\sqrt{2}} \\ \frac{v_2(h_2^D)_{31}}{\sqrt{2}} & \frac{v_2(h_2^D)_{32}}{\sqrt{2}} & \frac{v_2(h_2^D)_{33}}{\sqrt{2}} & \Omega_{34}^D v_2 \frac{v_\chi}{2\Lambda} & \Omega_{35}^D v_2 \frac{v_\chi}{2\Lambda} \\ \Omega_{41}^D v_2 \frac{v_\chi}{2\Lambda} & \Omega_{42}^D v_2 \frac{v_\chi}{2\Lambda} & \Omega_{43}^D v_2 \frac{v_\chi}{2\Lambda} & \frac{v_\chi(h_\chi^J)_{11}}{\sqrt{2}} & \frac{v_\chi(h_\chi^J)_{12}}{\sqrt{2}} \\ \Omega_{51}^D v_2 \frac{v_\chi}{2\Lambda} & \Omega_{52}^D v_2 \frac{v_\chi}{2\Lambda} & \Omega_{53}^D v_2 \frac{v_\chi}{2\Lambda} & \frac{v_\chi(h_\chi^J)_{21}}{\sqrt{2}} & \frac{v_\chi(h_\chi^J)_{22}}{\sqrt{2}} \end{pmatrix},$$

where mass eigenvalues can be written in general as:

$$m_d^2 = \frac{v_\chi^2 \left(\xi_{22} v_1^2 + \xi_{11} v_2^2 - \sqrt{4\xi_{12}^2 v_1^2 v_2^2 + (\xi_{22} v_1^2 - \xi_{11} v_2^2)^2} \right)}{8\Lambda^2}, \quad (53)$$

$$m_s^2 = \frac{v_\chi^2 \left(\xi_{22} v_1^2 + \xi_{11} v_2^2 + \sqrt{4\xi_{12}^2 v_1^2 v_2^2 + (\xi_{22} v_1^2 - \xi_{11} v_2^2)^2} \right)}{8\Lambda^2}, \quad (54)$$

$$m_b^2 = \frac{1}{2} v_2^2 \left((h_2^D)_{31}^2 + (h_2^D)_{32}^2 + (h_2^D)_{33}^2 \right), \quad (55)$$

$$m_{\mathcal{J}^1} = \frac{1}{4} v_\chi^2 \left(\rho - \sqrt{\rho^2 - 4\eta^2} \right), \quad (56)$$

$$m_{\mathcal{J}^2} = \frac{1}{4} v_\chi^2 \left(\rho + \sqrt{\rho^2 - 4\eta^2} \right), \quad (57)$$

and

$$\begin{aligned}
\xi_{11} &= \Omega_{11}^D \Omega_{12}^D + \Omega_{12}^D \Omega_{13}^D - \frac{(\Omega_{11}^D (h_2^D)_{31} + \Omega_{12}^D (h_2^D)_{32} + \Omega_{13}^D (h_2^D)_{33})^2}{(Y_d)_{3,1}^2 + (Y_d)_{3,2}^2 + (Y_d)_{3,3}^2}, \\
\xi_{22} &= \Omega_{21}^D \Omega_{22}^D + \Omega_{22}^D \Omega_{23}^D - \frac{(\Omega_{21}^D (h_2^D)_{31} + \Omega_{22}^D (h_2^D)_{32} + \Omega_{23}^D (h_2^D)_{33})^2}{(Y_d)_{3,1}^2 + (Y_d)_{3,2}^2 + (Y_d)_{3,3}^2}, \\
\xi_{12} &= \Omega_{11}^D \Omega_{21}^D + \Omega_{12}^D \Omega_{22}^D + \Omega_{13}^D \Omega_{23}^D - \frac{[(\Omega_{11}^D (h_2^D)_{31} + \Omega_{12}^D (h_2^D)_{32} + \Omega_{13}^D (h_2^D)_{33})(\Omega_{21}^D (h_2^D)_{31} + \Omega_{22}^D (h_2^D)_{32} + \Omega_{23}^D (h_2^D)_{33})]}{((Y_d)_{3,1}^2 + (Y_d)_{3,2}^2 + (Y_d)_{3,3}^2)}, \\
\rho &= (h_\chi^J)_{11})^2 + ((h_\chi^J)_{12})^2 + ((h_\chi^J)_{21})^2 + ((h_\chi^J)_{25}), \\
\eta &= (h_\chi^J)_{12}(h_\chi^J)_{21} - (h_\chi^J)_{11}(h_\chi^J)_{12}.
\end{aligned} \tag{58}$$

Furthermore, the rotation matrix for left-handed down quarks has an identical structure as up-quarks, it can be written as: $\mathbb{V}_L^D \approx \mathbb{V}_{L1}^D \mathbb{V}_{L2}^D$, where each matrix reads:

$$\mathbb{V}_{L1}^D \approx \begin{pmatrix} 1 & 0 & 0 & \frac{v_1 v_\chi}{2} \kappa_{12}^L & \frac{v_1 v_\chi}{2} \kappa_{11}^L \\ 0 & 1 & 0 & \frac{v_2 v_\chi}{2} \kappa_{22}^L & \frac{v_2 v_\chi}{2} \kappa_{21}^L \\ 0 & 0 & 1 & \frac{v_2 v_\chi}{2\sqrt{2}\Lambda} \kappa_{32}^L & \frac{v_2 v_\chi}{2\sqrt{2}\Lambda} \kappa_{31}^L \\ -\frac{v_1 v_\chi}{2} \kappa_{12}^L & -\frac{v_2 v_\chi}{2} \kappa_{22}^L & -\frac{v_2 v_\chi}{2\sqrt{2}\Lambda} \kappa_{32}^L & 1 & 0 \\ -\frac{v_1 v_\chi}{2} \kappa_{11}^L & -\frac{v_2 v_\chi}{2} \kappa_{21}^L & -\frac{v_2 v_\chi}{2\sqrt{2}\Lambda} \kappa_{31}^L & 0 & 1 \end{pmatrix}, \tag{59}$$

$$\mathbb{V}_{L2}^D \approx \begin{pmatrix} c_{ds} & s_{ds} & r_1^D & 0 & 0 \\ -s_{ds} & c_{ds} & r_2^D & 0 & 0 \\ -r_1^D c_{ds} + r_2^D s_{ds} & -r_2^D c_{ds} - r_1^D s_{ds} & 1 & 0 & 0 \\ 0 & 0 & 0 & 1 & 0 \\ 0 & 0 & 0 & 0 & 1 \end{pmatrix}, \tag{60}$$

with the parameters

$$\kappa_{ij}^L = \frac{1}{m_{\mathcal{J}^1} m_{\mathcal{J}^2}} (-Y_{i5} (h_\chi^J)_{j1} + Y_{i4} (h_\chi^J)_{j2}), \tag{61}$$

$$r_1^D = \frac{v_\chi v_2^2}{2\sqrt{2}\Lambda m_b^2} (\Omega_{11}^D (h_2^D)_{31} + \Omega_{12}^D (h_2^D)_{32} + \Omega_{13}^D (h_2^D)_{33}), \tag{62}$$

$$r_2^D = \frac{v_\chi v_1 v_2}{2\sqrt{2}\Lambda m_b^2} (\Omega_{21}^D (h_2^D)_{31} + \Omega_{22}^D (h_2^D)_{32} + \Omega_{23}^D (h_2^D)_{33}), \tag{63}$$

$$\tan \theta_{ds} = t_{ds} = \frac{v_1 v_2^3 \xi_{12}}{v_1^2 v_2^2 \xi_{22} - 4m_b^2 m_d^2}, \tag{64}$$

and Y_{ij} represents the Yukawa couplings in the $(\mathbb{M}_D)_{ij}$ entry of the mass matrix. For instance, $Y_{15} = (h_1^J)_2$ or $Y_{34} = \Omega_{34}^D$.

We can also get the rotation matrix elements through the CKM matrix, which is defined by $\mathbb{V}_{CKM} = \mathbb{V}_L^{U\dagger} \mathbb{V}_L^D$, so we can relate down-quarks phenomenology to the θ_{uc} angle in Eq. (43) as well.

On the other hand, the rotation matrix for right-handed down quarks has a more complicated structure, it can also be written as $\mathbb{V}_R^D \approx \mathbb{V}_{R1}^D \mathbb{V}_{R2}^D$ where the rotation matrices are defined as:

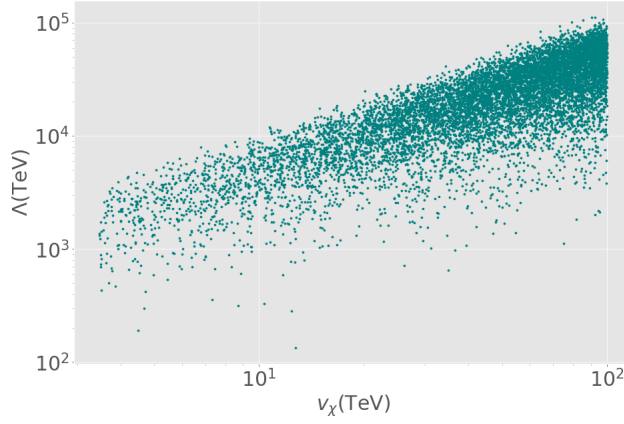


FIG. 4: Monte Carlo exploration for Λ as a function of v_χ according to the down and strange masses in Eq. (53) and Eq. (54) respectively.

$$\mathbb{V}_{R1}^D \approx \begin{pmatrix} 1 & 0 & 0 & -\frac{v_2 v_\chi^2}{2\sqrt{2}\Lambda} \kappa_{11}^R & -\frac{v_2 v_\chi^2}{2\sqrt{2}\Lambda} \kappa_{12}^R \\ 0 & 1 & 0 & -\frac{v_2 v_\chi^2}{2\sqrt{2}\Lambda} \kappa_{21}^R & -\frac{v_2 v_\chi^2}{2\sqrt{2}\Lambda} \kappa_{22}^R \\ 0 & 0 & 1 & -\frac{v_2 v_\chi^2}{2\sqrt{2}\Lambda} \kappa_{31}^R & -\frac{v_2 v_\chi^2}{2\sqrt{2}\Lambda} \kappa_{32}^R \\ \frac{v_2 v_\chi^2}{2\sqrt{2}\Lambda} \kappa_{11}^R & \frac{v_2 v_\chi^2}{2\sqrt{2}\Lambda} \kappa_{21}^R & \frac{v_2 v_\chi^2}{2\sqrt{2}\Lambda} \kappa_{31}^R & 1 & 0 \\ \frac{v_2 v_\chi^2}{2\sqrt{2}\Lambda} \kappa_{12}^R & \frac{v_2 v_\chi^2}{2\sqrt{2}\Lambda} \kappa_{22}^R & \frac{v_2 v_\chi^2}{2\sqrt{2}\Lambda} \kappa_{32}^R & 0 & 1 \end{pmatrix}, \quad (65)$$

$$\mathbb{V}_{R2}^D \approx \begin{pmatrix} c_{13} & 0 & -s_{13} & 0 & 0 \\ 0 & 1 & 0 & 0 & 0 \\ s_{13} & 0 & c_{13} & 0 & 0 \\ 0 & 0 & 0 & 1 & 0 \\ 0 & 0 & 0 & 0 & 1 \end{pmatrix} \begin{pmatrix} 1 & 0 & 0 & 0 & 0 \\ 0 & c_{23} & -s_{23} & 0 & 0 \\ 0 & s_{23} & c_{23} & 0 & 0 \\ 0 & 0 & 0 & 1 & 0 \\ 0 & 0 & 0 & 0 & 1 \end{pmatrix} \begin{pmatrix} c_{12} & s_{12} & 0 & 0 & 0 \\ -s_{12} & c_{12} & 0 & 0 & 0 \\ 0 & 0 & 1 & 0 & 0 \\ 0 & 0 & 0 & 1 & 0 \\ 0 & 0 & 0 & 0 & 1 \end{pmatrix}, \quad (66)$$

where

$$\kappa_{ij}^R = \Omega_{4i}^D (h_\chi^J)_{1j} + \Omega_{5i}^D (h_\chi^J)_{2j}, \quad (67)$$

$$t_{13} = \frac{(h_2^D)_{31}}{(h_2^D)_{33}}, \quad (68)$$

$$t_{23} = \frac{(h_2^D)_{32}}{\sqrt{((h_2^D)_{31})^2 + ((h_2^D)_{32})^2 + ((h_2^D)_{33})^2}}, \quad (69)$$

$$\begin{aligned} t_{12} &\approx s_{12} \\ &= \frac{v_\chi^2}{4\Lambda^2 m_s^2} \left(\frac{\Omega_{22}^D v_1^2 (\Omega_{21}^D (h_2^D)_{33} - \Omega_{23}^D (h_2^D)_{31})}{\sqrt{(Y_d)_{3,1}^2 + (Y_d)_{3,2}^2 + (Y_d)_{3,3}^2}} + \frac{\Omega_{12}^D v_2^2 (\Omega_{11}^D (h_2^D)_{33} - \Omega_{13}^D (h_2^D)_{31})}{\sqrt{(Y_d)_{3,1}^2 + (Y_d)_{3,2}^2 + (Y_d)_{3,3}^2}} \right) \\ &\quad + s_{23} [((\Omega_{23}^{D2} - \Omega_{21}^{D2}) v_1^2 + (\Omega_{13}^{D2} - \Omega_{11}^{D2}) v_2^2) s_{13} c_{13} + (\Omega_{21}^D \Omega_{23}^D v_1^2 + \Omega_{11}^D \Omega_{13}^D v_2^2) (s_{13}^2 - c_{13}^2)]. \end{aligned} \quad (70)$$

Finally, since we have two particle masses obtained by effective operators, we give an uniformly distributed random value to all Ω_{ij}^D parameters in the interval $[1, 10]$ excepting Ω_{11}^D . Ω_{11}^D and Λ are unknowns whose value fix the bottom and strange masses so the set of equations was numerically solved for them and only solutions consistent with the condition $\Omega_{11}^D < 10$ were taken. The allowed values for Λ as a function of v_χ are shown in figure 4, where an upper bound of $\Lambda \leq \left(\frac{v_2}{2\sqrt{2}m_d} 0.063 \right) v_\chi \approx 4.7 v_\chi$ has been found.

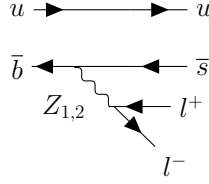
Fermion	Λ upper bound
e	$\Lambda \leq \sqrt[3]{9.4 \frac{v_2}{4m_e} v_\chi} \approx 17v_\chi$
u	$\Lambda \leq \frac{5v_1}{m_u} v_\chi \approx 5.6 \times 10^5 v_\chi$
d, s	$\Lambda \leq \left(\frac{v_2}{2\sqrt{2}m_d} 0.063 \right) v_\chi \approx 4.7v_\chi$

TABLE III: Λ scale upper bound according to each light fermion mass.

The upper bounds for Λ is summarized in table III. It can be seen that the down quark sector yields the smallest upper bound, meaning that SM fermion masses restrict the effective operators energy scale to $\Lambda \leq 4.7v_\chi$.

VII. B MESON ANOMALIES

The B meson anomaly measured at LHCb [14] can be understood in this model by considering flavor changing neutral interaction mediated by Z_1 and Z_2 , according to the diagram shown in figure 5.

FIG. 5: Decay $B^+ \rightarrow K^+ \ell^+ \ell^-$ due to neutral gauge bosons Z_1 and Z_2 .

The relevant interactions arise from kinetic terms of particles, giving the Z_1 and Z_2 interactions in terms of the particle isospin T_3 and electric charge Q according to:

$$g \left(-\frac{1}{c_W} (T_3 - s_W^2 Q) c_Z - \frac{g_X}{g} X s_Z \right) Z_1^\mu + g \left(\frac{1}{c_W} (T_3 - s_W^2 Q) s_Z - \frac{g_X}{g} X c_Z \right) Z_2^\mu, \quad (71)$$

so the interaction Lagrangian among particles can be written as:

$$\mathcal{L}_{ij} = ig \bar{f}_{Li} [J_i^{L1} \not{Z}_1 + J_i^{L2} \not{Z}_2] f_{Li} + ig \bar{f}_{Ri} [J_i^{R1} \not{Z}_1 + J_i^{R2} \not{Z}_2] f_{Ri}, \quad (72)$$

where f_i runs over all particles in the flavor basis and the $J_i^{L1,2}$, $J_i^{R1,2}$ couplings can be read from table IV and V.

f_{Li}	J_i^{L1}	J_i^{L2}
u_L^1	$\frac{1}{c_W} \left(-\frac{1}{2} + \frac{2}{3} s_W^2 \right) c_Z - \frac{g_X}{3g} s_Z$	$-\frac{1}{c_W} \left(-\frac{1}{2} + \frac{2}{3} s_W^2 \right) s_Z - \frac{g_X}{3g} c_Z$
$u_L^{2,3}$	$\frac{1}{c_W} \left(-\frac{1}{2} + \frac{2}{3} s_W^2 \right) c_Z$	$-\frac{1}{c_W} \left(-\frac{1}{2} + \frac{2}{3} s_W^2 \right) s_Z$
d_L^1	$\frac{1}{c_W} \left(\frac{1}{2} - \frac{1}{3} s_W^2 \right) c_Z - \frac{g_X}{3g} s_Z$	$-\frac{1}{c_W} \left(\frac{1}{2} - \frac{1}{3} s_W^2 \right) s_Z - \frac{g_X}{3g} c_Z$
$d_L^{2,3}$	$\frac{1}{c_W} \left(\frac{1}{2} - \frac{1}{3} s_W^2 \right) c_Z$	$-\frac{1}{c_W} \left(\frac{1}{2} - \frac{1}{3} s_W^2 \right) s_Z$
$e_L^{e,\mu}$	$\frac{1}{c_W} \left(\frac{1}{2} - s_W^2 \right) c_Z$	$-\frac{1}{c_W} \left(\frac{1}{2} - s_W^2 \right) s_Z$
e_L^τ	$\frac{1}{c_W} \left(\frac{1}{2} - s_W^2 \right) c_Z + \frac{g_X}{g} s_Z$	$-\frac{1}{c_W} \left(\frac{1}{2} - s_W^2 \right) s_Z + \frac{g_X}{g} c_Z$
E_L	$-\frac{s_W^2}{c_W} c_Z + \frac{g_X}{g} s_Z$	$\frac{s_W^2}{c_W} s_Z + \frac{g_X}{g} c_Z$
\mathcal{T}_L	$\frac{2s_W^2}{3c_W} c_Z - \frac{g_X}{3g} s_Z$	$-\frac{2s_W^2}{3c_W} s_Z - \frac{g_X}{3g} c_Z$
\mathcal{J}_L^a	$-\frac{s_W^2}{3c_W} c_Z$	$\frac{s_W^2}{3c_W} s_Z$

TABLE IV: Neutral current couplings for left-handed fermions.

f_{Ri}	J_i^{R1}	J_i^{R2}
$U_R^{1,2,3}$	$\frac{2s_W^2}{3c_W}c_Z - \frac{2g_X}{3g}s_Z$	$-\frac{2s_W^2}{3c_W}s_Z - \frac{2g_X}{3g}c_Z$
$D_R^{1,2,3}$	$-\frac{s_W^2}{3c_W}c_Z + \frac{g_X}{3g}s_Z$	$\frac{s_W^2}{3c_W}s_Z + \frac{g_X}{3g}c_Z$
$e_R^{e,\tau}$	$-\frac{s_W^2}{c_W}c_Z + \frac{4g_X}{3g}s_Z$	$\frac{s_W^2}{c_W}s_Z + \frac{4g_X}{3g}c_Z$
e_R^μ	$-\frac{s_W^2}{c_W}c_Z + \frac{g_X}{3g}s_Z$	$\frac{s_W^2}{c_W}s_Z + \frac{g_X}{3g}c_Z$
E_R	$-\frac{s_W^2}{c_W}c_Z + \frac{2g_X}{3g}s_Z$	$\frac{s_W^2}{c_W}s_Z + \frac{2g_X}{3g}c_Z$
\mathcal{T}_R	$\frac{2s_W^2}{3c_W}c_Z - \frac{2g_X}{3g}s_Z$	$-\frac{2s_W^2}{3c_W}s_Z - \frac{2g_X}{3g}c_Z$
\mathcal{J}_R^a	$-\frac{s_W^2}{3c_W}c_Z + \frac{g_X}{3g}s_Z$	$\frac{s_W^2}{3c_W}s_Z + \frac{g_X}{3g}c_Z$

TABLE V: Neutral current couplings for right-handed fermions.

In general, the Z_2^μ couplings can be obtained by changing the sign to the electroweak term of Z_1^μ (the first term) and by doing the replacement $s_Z \leftrightarrow c_Z$. Finally, by rotating the fermions into mass eigenstates F_m , the interaction Lagrangian becomes:

$$\mathcal{L}_{mn} = ig\bar{F}_{Lm}(\mathbb{V}_L^\dagger)^{mi}[J_i^{L1}\not{Z}_1 + J_i^{L2}\not{Z}_2](\mathbb{V}_L)^{in}F_{Ln} + \bar{F}_{Rm}(\mathbb{V}_R^\dagger)^{mi}[J_i^{R1}\not{Z}_1 + J_i^{R2}\not{Z}_2](\mathbb{V}_R)^{in}F_{Rn}. \quad (73)$$

A. $b \rightarrow s\ell^+\ell^-$ coupling

From the Lagrangian in Eq. (73), we take the case $m = 2$ and $n = 3$ for the down quark sector to extract the down-strange flavor changing interaction. First, from table V we see that there is a right-handed down-like universality, so its contribution to the flavor changing Lagrangian vanishes due to the unitarity of the rotation matrix, $(\mathbb{V}_R^{D\dagger})^{mi}(\mathbb{V}_R^D)^{in} = \delta_{mn}$. Second, for the left-handed particles we can split the couplings into SM and exotic terms as:

$$(\mathbb{V}_L^{D\dagger})^{2i}J_i^{Ll}(\mathbb{V}_L^D)^{i3} = (\mathbb{V}_L^{D\dagger})^{21}J_1^{Ll}(\mathbb{V}_L^D)^{13} + (\mathbb{V}_L^{D\dagger})^{2r}J_r^{Ll}(\mathbb{V}_L^D)^{r3} + (\mathbb{V}_L^{D\dagger})^{2\alpha}J_\alpha^{Ll}(\mathbb{V}_L^D)^{\alpha3}, \quad (74)$$

where $r = 2, 3$ labels the second and third generation quarks, $\alpha = 4, 5$ labels the exotic quarks and $l = 1, 2$ label the neutral gauge bosons. Then, from table IV, we can see that $J_2^{L1,2} = J_3^{L1,2}$. Thus, we can use the unitarity constraint to replace:

$$(\mathbb{V}_L^{D\dagger})^{2r}(\mathbb{V}_L^D)^{r3} = -(\mathbb{V}_L^{D\dagger})^{21}(\mathbb{V}_L^D)^{13} - (\mathbb{V}_L^{D\dagger})^{2\alpha}(\mathbb{V}_L^D)^{\alpha3}, \quad (75)$$

so finally the interaction Lagrangian can be written as:

$$\begin{aligned} \mathcal{L}_{bs} &= \bar{s}[g(\mathbb{V}_L^{D\dagger})^{21}(J_1^{L1} - J_r^{L1})(\mathbb{V}_L^D)^{13}\not{Z}_l]P_L b + \bar{s}[g(\mathbb{V}_L^{D\dagger})^{2\alpha}(J_\alpha^{L2} - J_r^{L1})(\mathbb{V}_L^D)^{\alpha3}\not{Z}_l]P_L b \\ &= \bar{s}g(\mathbb{V}_L^{D\dagger})^{21}\left(-\frac{1}{3}\frac{g_X}{g}(s_Z\delta_{l1} + c_Z\delta_{l2})\right)(\mathbb{V}_L^D)^{13}\not{Z}_l P_L b + \bar{s}g(\mathbb{V}_L^{D\dagger})^{2\alpha}\left(-\frac{1}{2}\frac{s_Z}{g}\right)(\mathbb{V}_L^D)^{\alpha3}\not{Z}_l P_L b. \end{aligned} \quad (76)$$

It can be seen that the second term is proportional to s_Z for both Z_1 and Z_2 which initially suppresses the contribution. Additionally, the rotation matrix entries $(\mathbb{V}_L^D)^{\alpha3}$ and $(\mathbb{V}_L^{D\dagger})^{2\alpha}$ comes from the seesaw decoupling of exotic quarks to SM quarks, so they are proportional to $v_\chi/m_{\mathcal{J}^1}m_{\mathcal{J}^2}$ GeV⁻¹ which further suppress the term, so we can neglect it. Finally, the bottom-strange interaction Lagrangian reads:

$$\begin{aligned} \mathcal{L}_{bZs} &= -(\mathbb{V}_L^D)_{12}^*(\mathbb{V}_L^D)_{13}\left(\frac{g_X}{3}s_Z\right)\bar{s}\not{Z}_1 P_L b - (\mathbb{V}_L^D)_{12}^*(\mathbb{V}_L^D)_{13}\left(\frac{g_X}{3}c_Z\right)\bar{s}\not{Z}_2 P_L b \\ &\equiv g_X g_{bs}^1 \bar{s}\not{Z}_1 P_L b + g_X g_{bs}^2 \bar{s}\not{Z}_2 P_L b, \end{aligned} \quad (77)$$

where

$$\begin{aligned} (\mathbb{V}_L^D)_{13} &= r_1^D \\ &\approx ((\mathbb{V}_{CKM})_{13}c_{uc} + (\mathbb{V}_{CKM})_{23}s_{uc}), \end{aligned} \quad \begin{aligned} (\mathbb{V}_L^D)_{12}^* &= \sin\theta_{ds} = s_{ds} \\ &\approx ((\mathbb{V}_{CKM})_{12}^*c_{uc} + (\mathbb{V}_{CKM})_{22}^*s_{uc}), \end{aligned} \quad (78)$$

where $g_{bs}^2 = c_Z/3$, \mathbb{V}_{CKM} represents the CKM matrix, r_1^D and θ_{ds} are defined in Eqs. (62) and (64), respectively, while $s_{uc} = \sin\theta_{uc}$ and $c_{uc} = \cos\theta_{uc}$ are defined through Eq. (43). Additionally, Eq. (77) tell us that the $b \rightarrow s$ transition is possible by the interaction with Z_1^μ and Z_2^μ , but the Z_1^μ interaction is suppressed by s_Z , making it about two orders of magnitude smaller than the Z_2^μ interaction, so we can neglect it.

B. $Z^\alpha \ell^+ \ell^-$ coupling

By considering the general neutral current Lagrangian from Eq. (73) for the case of charged leptons and $m = n = 1, 2$, it can be written as:

$$\mathcal{L} = ig\bar{e}^p \not{Z}_l [(\mathbb{V}_L^{E\dagger})^{pi} J_i^{Ll} (\mathbb{V}_L^E)^{ip} P_L + (\mathbb{V}_R^{E\dagger})^{pi} J_i^{Rl} (\mathbb{V}_R^E)^{ip} P_R] e^p, \quad (79)$$

where $p = e, \mu$ labels the electron and muon mass eigenstate and $l = 1, 2$ labels the neutral gauge boson. For the left-handed coupling, we expand the index i as:

$$(\mathbb{V}_L^{E\dagger})^{pi} J_i^{Ll} (\mathbb{V}_L^E)^{ip} = (\mathbb{V}_L^{E\dagger})^{pp'} J_{p'}^{Ll} (\mathbb{V}_L^E)^{p'p} + (\mathbb{V}_L^{E\dagger})^{p\tau} J_\tau^{Ll} (\mathbb{V}_L^E)^{\tau p} + (\mathbb{V}_L^{E\dagger})^{pE} J_E^{Ll} (\mathbb{V}_L^E)^{Ep}, \quad (80)$$

where $p' = e, \mu$ as well, but it represents a sum over the index different from p that just labels the mass eigenstate. Since $J_e^{Ll} = J_\mu^{Ll}$, as it can be seen from table IV, we can factor $J_{s'}^{Ll}$ and apply the unitarity constraint to obtain:

$$(\mathbb{V}_L^{E\dagger})^{pp'} (\mathbb{V}_L^E)^{p'p} = 1 - (\mathbb{V}_L^{E\dagger})^{p\tau} (\mathbb{V}_L^E)^{\tau p} - (\mathbb{V}_L^{E\dagger})^{pE} (\mathbb{V}_L^E)^{Ep}, \quad (81)$$

so that the Lagrangian reads:

$$\begin{aligned} \mathcal{L} &= ig\bar{e}^p \not{Z}_l [(J_{p'}^{Ll} + (\mathbb{V}_L^{E\dagger})^{p\tau} (J_\tau^{Ll} - J_{p'}^{Ll}) (\mathbb{V}_L^E)^{\tau p} + (\mathbb{V}_L^{E\dagger})^{pE} (J_E^{Ll} - J_{p'}^{Ll}) (\mathbb{V}_L^E)^{Ep})] P_L + (\mathbb{V}_R^{E\dagger})^{pi} J_i^{Rl} (\mathbb{V}_R^E)^{ip} P_R] e^p \quad (82) \\ &= ig\bar{e}^p \not{Z}_l \left[\left(J_{p'}^{Ll} + \left(\frac{g_X}{g} (s_Z \delta_{l1} + c_Z \delta_{l2}) \right) |(\mathbb{V}_L^E)^{\tau p}|^2 + \left(-\frac{c_Z \delta_{l1} + s_Z \delta_{l2}}{2c_W} + \frac{g_X}{g} (s_Z \delta_{l1} + c_Z \delta_{l2}) \right) |(\mathbb{V}_L^E)^{Ep}|^2 \right) P_L \right. \\ &\quad \left. + (\mathbb{V}_R^{E\dagger})^{pi} J_i^{Rl} (\mathbb{V}_R^E)^{ip} P_R \right] e^p. \quad (83) \end{aligned}$$

The entries (4, 1) and (4, 2) of the charged lepton rotation matrix comes from the seesaw decoupling of the exotic lepton E , so as it can be seen in Eq. (30) it is suppressed by m_E^{-1} and we can neglect it. Likewise, we neglect the term proportional to $|(\mathbb{V}_L^E)^{\tau s}|$ because such entries come from the seesaw decoupling of the τ particle and then suppressed by $(v_\chi/\Lambda)^3$. In this way, the interaction Lagrangian simplifies to:

$$\mathcal{L} = ig\bar{e}^s \not{Z}_l \left[\left(\frac{c_Z \delta_{l1} - s_Z \delta_{l2}}{c_W} \left(\frac{1}{2} - s_W^2 \right) \right) P_L + (\mathbb{V}_R^{E\dagger})^{si} J_i^{Rl} (\mathbb{V}_R^E)^{is} P_R \right] e^s. \quad (84)$$

We proceed in a similar fashion for the right-handed coupling by expanding the index i as:

$$(\mathbb{V}_R^{E\dagger})^{pi} J_i^{Rl} (\mathbb{V}_R^E)^{ip} = (\mathbb{V}_R^{E\dagger})^{pa} J_a^{Rl} (\mathbb{V}_R^E)^{ap} + (\mathbb{V}_R^{E\dagger})^{p\mu} J_\mu^{Rl} (\mathbb{V}_R^E)^{\mu p} + (\mathbb{V}_R^{E\dagger})^{pE} J_E^{Rl} (\mathbb{V}_R^E)^{Ep}, \quad (85)$$

where $a = e, \tau$. Then we can factor the coupling J_a^{Rl} and apply the unitarity constraint to rewrite the Lagrangian as:

$$\mathcal{L} = ig\bar{e}^s \not{Z}_l \left[\left(\frac{c_Z \delta_{l1} - s_Z \delta_{l2}}{c_W} \left(\frac{1}{2} - s_W^2 \right) \right) P_L + (J_p^{Rl} + (J_\mu^{Rl} - J_p^{Rl}) |(\mathbb{V}_R^E)^{\mu s}|^2 + (J_E^{Rl} - J_p^{Rl}) |(\mathbb{V}_R^E)^{Es}|^2) P_R \right] e^s. \quad (86)$$

According to Eq. (30), we can neglect the term proportional to $|(\mathbb{V}_R^E)^{Ep}|^2$ because such entry of the rotation matrix is suppressed by m_E^{-2} . Likewise we can neglect $|(\mathbb{V}_R^E)^{\mu e}|^2$ while $|(\mathbb{V}_R^E)^{\mu\mu}|^2 \approx 1$, making two different couplings for electron and muon, as expected from non-universality. So the interaction Lagrangian can be approximated to:

$$\mathcal{L} = ig\bar{e}^s \not{Z}_l \left[\left(\frac{c_Z \delta_{l1} - s_Z \delta_{l2}}{c_W} \left(\frac{1}{2} - s_W^2 \right) \right) P_L + \left(\frac{gs_W^2}{c_W} (-c_Z \delta_{l1} + s_Z \delta_{l2}) + \left(\frac{4g_X}{3g} - \frac{g_X}{g} \delta_{\mu s} \right) (s_Z \delta_{l1} + c_Z \delta_{l2}) \right) P_R \right] e^s. \quad (87)$$

Finally, the Z_1^μ gauge boson has the same neutral SM couplings times a factor $c_Z \approx 1$, so its contribution is already included in the SM prediction to the B^+ decay. Therefore, we only take the Z_2 interaction, which gives:

$$\begin{aligned}\mathcal{L}_{Z\ell\ell} &= \bar{e}\not{Z}_2 \left[-\frac{g(1-2s_W^2)s_Z}{2c_W} P_L + \left(\frac{gs_W^2}{c_W} s_Z + \frac{4g_X}{3} \right) P_R \right] e + \bar{\mu}\not{Z}_2 \left[-\frac{g(1-2s_W^2)s_Z}{2c_W} P_L + \left(\frac{gs_W^2}{c_W} s_Z + \frac{g_X}{3} \right) P_R \right] \mu \\ &\approx \bar{e}\not{Z}_2 \left[\frac{4g_X}{3} P_R \right] e + \bar{\mu}\not{Z}_2 \left[\frac{g_X}{3} P_R \right] \mu \\ &\equiv g_X g_{Zee}^R \bar{e}\not{Z}_2 P_R e + g_X g_{Z\mu\mu}^R \bar{\mu}\not{Z}_2 P_R \mu,\end{aligned}\tag{88}$$

being such interaction Lagrangians in agreement with [31] and showing that the interaction of the Z_2^μ gauge boson to left-handed leptons is highly suppressed while interaction to right-handed leptons depends directly on g_X . At low energies, the momentum transfer by means of intermediary particles is negligible, which makes the decay to be derived from the following effective Hamiltonian:

$$\begin{aligned}\mathcal{H}_{\text{eff}}^{NP} &= \frac{g_X^2}{M_{Z_2}^2} [\bar{s} (g_{bs}^2 P_L) b] [\bar{\ell}_a \gamma^\mu (g_{Z\ell_a\ell_a}^R P_R) \ell_a] + \text{H.C.} \\ &= \frac{9}{v_\chi^2} [\bar{s} (g_{bs}^2 P_L) b] [\bar{\ell}_a \gamma^\mu (g_{Z\ell_a\ell_a}^R P_R) \ell_a] + \text{H.C.},\end{aligned}\tag{89}$$

where $\ell_a = (e, \mu)$ and $M_{Z_2} \approx M_{Z'} = g_X v_\chi / 3$ according to Eq. (23). Although, it is worth to notice that such operator is g_X independent and is also suppressed by v_χ . Such an operator affects the ordinary SM contribution which can be described through the Wilson operators \mathcal{C}_9 and \mathcal{C}_{10} [32]:

$$\mathcal{H}_{\text{eff}}^{\text{SM}} = -\frac{G_F \alpha_{\text{em}}}{\sqrt{2}\pi} \mathbb{V}_{tb} V_{ts}^* \sum_i \left[C_i^{\text{SM}} \mathcal{O}_i + C_i'^{\text{SM}} \mathcal{O}'_i \right] + \text{H.c.},\tag{90}$$

where $C_9^{\text{SM}} \approx 4.053$, $C_{10}^{\text{SM}} \approx -4.189$ obtained from flavio [33], $C_9'^{\text{SM}} = C_{10}'^{\text{SM}} = 0$, $\frac{G_F \alpha_{\text{em}}}{\sqrt{2}\pi} \mathbb{V}_{tb} V_{ts}^* \approx \frac{1}{(36\text{TeV})^2}$ and

$$\mathcal{O}_9 = [\bar{s} \gamma_\mu P_L b] [\bar{\ell}_a \gamma^\mu \ell_a], \quad \mathcal{O}_{10} = [\bar{s} \gamma_\mu P_L b] [\bar{\ell}_a \gamma^\mu \gamma_5 \ell_a].\tag{91}$$

$$\mathcal{O}'_9 = [\bar{s} \gamma_\mu P_R b] [\bar{\ell}_a \gamma^\mu \ell_a], \quad \mathcal{O}'_{10} = [\bar{s} \gamma_\mu P_R b] [\bar{\ell}_a \gamma^\mu \gamma_5 \ell_a].\tag{92}$$

By putting together both effective Hamiltonians in Eqs. (89) and (90) we obtain the total effective Hamiltonian:

$$\mathcal{H}_{\text{eff}} = \mathcal{H}_{\text{eff}}^{\text{SM}} + \mathcal{H}_{\text{eff}}^{NP}\tag{93}$$

$$\begin{aligned}&= -\frac{1}{(36\text{TeV})^2} \left[C_9^{\text{SM}} - \frac{9(36\text{TeV})^2}{2v_\chi^2} g_{bs}^2 g_{Z\ell_a\ell_a}^R \right] \mathcal{O}_9 - \frac{1}{(36\text{TeV})^2} \left[C_{10}^{\text{SM}} - \frac{9(36\text{TeV})^2}{2v_\chi^2} g_{bs}^2 g_{Z\ell_a\ell_a}^R \right] \mathcal{O}_{10} \\ &\equiv \mathcal{C}_9^{\ell_a} \mathcal{O}_9 + \mathcal{C}_{10}^{\ell_a} \mathcal{O}_{10},\end{aligned}\tag{94}$$

where the corrected Wilson coefficients are defined as:

$$\mathcal{C}_9^{\ell_a} = C_9^{\text{SM}} + \frac{3(36\text{TeV})^2 (\mathbb{V}_L^D)_{12}^* (\mathbb{V}_L^D)_{13}}{2v_\chi^2} g_{Z\ell_a\ell_a}^R, \quad \mathcal{C}_{10}^{\ell_a} = C_{10}^{\text{SM}} + \frac{3(36\text{TeV})^2 (\mathbb{V}_L^D)_{12}^* (\mathbb{V}_L^D)_{13}}{2v_\chi^2} g_{Z\ell_a\ell_a}^R,\tag{95}$$

$$\mathcal{C}_9'^{\ell_a} = C_9'^{\text{SM}} \quad \mathcal{C}_{10}'^{\ell_a} = C_{10}'^{\text{SM}}\tag{96}$$

being $g_{Zee}^R = 4/3$ and $g_{Z\mu\mu}^R = 1/3$ as defined in Eq. (88) while $g_{bs}^2 = -(\mathbb{V}_L^D)_{12}^* (\mathbb{V}_L^D)_{13}/3$ was used, according to its definition in Eq. (77).

C. B meson decays

The considered effective operators \mathcal{O}_9 and \mathcal{O}_{10} in Eq. (92) are related to some important and well measured decays. In particular, it is of our interest to show the consistency with B meson decays through the relative branching ratios

R_K and R_{K^*} , and to the branching ratio $\mathcal{B}[B_s \rightarrow \mu^+ \mu^-]$. To start, we can consider the decay $B^+ \rightarrow K^+ \ell^+ \ell^-$ whose relative branching fraction in the dilepton mass-squared range $1.1 \leq q^2 \leq 6 \text{ GeV}^2/c^4$ can be written as:

$$R_K = \frac{\int_{q_{\min}^2}^{q_{\max}^2} \frac{d\mathcal{B}[B^+ \rightarrow K^+ \mu^+ \mu^-]}{dq^2} dq^2}{\int_{q_{\min}^2}^{q_{\max}^2} \frac{d\mathcal{B}[B^+ \rightarrow K^+ e^+ e^-]}{dq^2} dq^2}, \quad (97)$$

which in terms of the Wilson coefficients can be rewritten as [34, 35]:

$$R_K = \frac{|C_9^{(\mu)} + C_9^{\prime(\mu)}|^2 + |C_{10}^{(\mu)} + C_{10}^{\prime(\mu)}|^2}{|C_9^{(e)} + C_9^{\prime(e)}|^2 + |C_{10}^{(e)} + C_{10}^{\prime(e)}|^2} \quad (98)$$

$$= \frac{|C_9^{(\mu)}|^2 + |C_{10}^{(\mu)}|^2}{|C_9^{(e)}|^2 + |C_{10}^{(e)}|^2}, \quad (99)$$

where SM contributions from the electromagnetic dipole operator, non-factorizable contributions from the weak effective Hamiltonian and the contribution due to C_9' and C_{10}' are neglected. Such formula can be explored to show consistency between the model and the recent experimental results reported by the LHCb collaboration [14] $R_K^{exp} = 0.846_{-0.041}^{+0.044}$ together with the prediction calculated by the Flavio package [33], as shown in figure 6 for different values of v_χ .

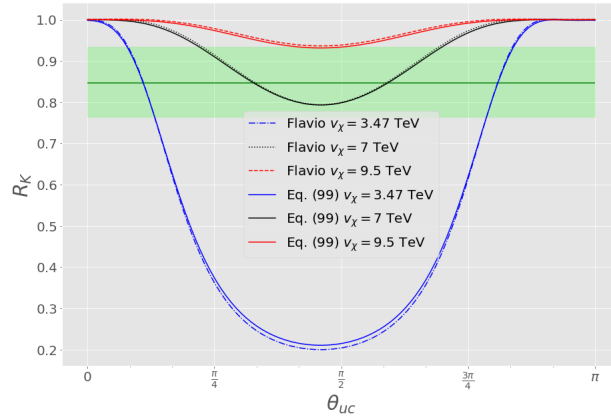


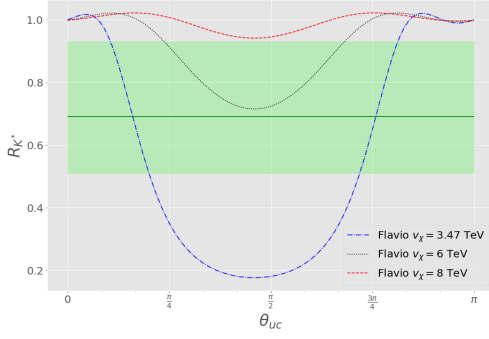
FIG. 6: Relative branching fraction R_K as a function of the up-charm mixing angle. The green shaded region represents the experimental value at 2σ C.L..

Since there are values of the curve inside the green shaded region, it sets an upper bound $v_\chi \leq 9.5 \text{ TeV}$ (red curves) from the Flavio prediction, where the maximum value of 9.5 TeV is allowed only for the single value of $\theta_{uc} = \pi/2$. For smaller values of v_χ , such as $v_\chi = 7 \text{ TeV}$ (black curves) or $v_\chi = 3.47 \text{ TeV}$ (blue curves), it sets an allowed region for θ_{uc} inside the allowed region shaded in green in figure 6.

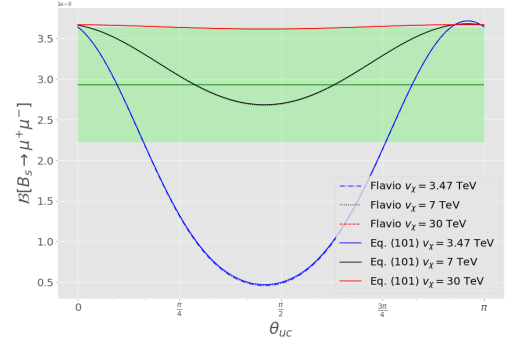
Additionally, we can consider the model compatibility to other observables such as R_{K^*} and the branching ratio $\mathcal{B}[B_s \rightarrow \mu^+ \mu^-]$ which can be obtained from the same Wilson coefficients. On the one hand, the B meson decay to a vector resonance K^* has its relative branching ratio definition in analogy to Eq. (97), in the dilepton mass-squared range $1.1 \leq q^2 \leq 6 \text{ GeV}^2/c^4$, as:

$$R_{K^*} = \frac{\int_{q_{\min}^2}^{q_{\max}^2} \frac{d\mathcal{B}[B^+ \rightarrow K^{*+} \mu^+ \mu^-]}{dq^2} dq^2}{\int_{q_{\min}^2}^{q_{\max}^2} \frac{d\mathcal{B}[B^+ \rightarrow K^{*+} e^+ e^-]}{dq^2} dq^2}. \quad (100)$$

However, due to the lack of a simple theoretical formula in terms of Wilson coefficients we present the relative branching ratio as obtained from flavio in figure 7a together with the 2σ C.L. region set by the experimental bound $R_{K^*}^{exp} = 0.69_{-0.09}^{+0.12}$ by the LHCb collaboration [15].



(a) Relative branching fraction R_{K^*} as a function of the up-charm mixing angle.



(b) Branching fraction $\mathcal{B}[B_s \rightarrow \mu^+ \mu^-]$ as a function of the up-charm mixing angle.

FIG. 7: R_{K^*} and $\mathcal{B}[B_s \rightarrow \mu^+ \mu^-]$ predictions of the $U(1)_X$ extension. The green shaded region represents the experimental value at 2σ C.L.

On the other hand, the branching ratio $\mathcal{B}[B_s \rightarrow \mu^+ \mu^-]$ relative to the SM prediction can be written in a good approximation in terms of the Wilson coefficients as [35]:

$$\begin{aligned} \mathcal{B}[B_s \rightarrow \mu^+ \mu^-] &= \left| \frac{C_{10}^{(\mu)} - C_{10}^{\prime(\mu)}}{C_{10}^{(\mu)SM} - C_{10}^{\prime(\mu)SM}} \right|^2 \mathcal{B}[B_s \rightarrow \mu^+ \mu^-]_{SM} \\ &= \left| \frac{C_{10}^{(\mu)}}{C_{10}^{(\mu)SM}} \right|^2 \mathcal{B}[B_s \rightarrow \mu^+ \mu^-]_{SM}, \end{aligned} \quad (101)$$

where the SM prediction is $\mathcal{B}[B_s \rightarrow \mu^+ \mu^-]_{SM} = (3.66 \pm 0.14) \times 10^{-9}$ [17] and coincides with the prediction of the flavio package while the current experimental world average is $\mathcal{B}[B_s \rightarrow \mu^+ \mu^-]_{exp} = (2.93 \pm 0.35) \times 10^{-9}$ [16].

It can be seen that the R_{K^*} prediction shown in figure 7a imposes a stringent bound on v_χ of $v_\chi \leq 8$ TeV while the branching ratio of the B_s meson to a di-muon pair in figure 7b does not restrict further such VEV, allowing values up to 30 TeV. However, both observables show a larger allowed region for θ_{uc} in comparison to the R_K prediction.

Observable	v_χ upper bound
R_K	$v_\chi \leq 9.5$ TeV
R_{K^*}	$v_\chi \leq 8$ TeV
$\mathcal{B}[B_s \rightarrow \mu^+ \mu^-]$	$v_\chi \leq 30$ TeV

TABLE VI: v_χ and θ_{uc} bound from R_K , R_{K^*} and $\mathcal{B}[B_s \rightarrow \mu^+ \mu^-]$ experimental data.

On the whole, the bounds on v_χ are summarized in table VI, which shows that the $U(1)_X$ extension is consistent with all three observables for $v_\chi \leq 8$ TeV while figures 6 and 7b shows the accuracy of the theoretical formulas shown in Eqs. (99) and (101) in comparison to the flavio prediction. Moreover, a lower bound for v_χ can be obtained if we accept the g_X value on the perturbative limit of $\sqrt{4\pi}$, which together with the experimental Z' lower bound on the mass of $m_{Z_2} > 4.1$ TeV by the ATLAS collaboration and the mass expression of Eq. (23), we obtain the following lower bound on v_χ :

$$\begin{aligned} 4.1 \text{ TeV} &\leq \frac{g_X v_\chi}{3} < \frac{\sqrt{4\pi} v_\chi}{3} \\ v_\chi &\geq 3.47 \text{ TeV}. \end{aligned} \quad (102)$$

Then, putting it all together we find that v_χ has to be on the interval:

$$3.47 \text{ TeV} \leq v_\chi \leq 8 \text{ TeV}, \quad (103)$$

which means that there is an upper bound for the mass of the Z_2^μ gauge boson of $m_{Z_2} \leq \frac{\sqrt{4\pi} 8}{3} \text{ TeV} \approx 9.5 \text{ TeV}$.

Furthermore, restrictions on θ_{uc} also affect the θ_{ds} angle due to the CKM matrix. From Eqs. (59), (60) and (44) we can calculate the CKM matrix as $\mathbb{V}_{CKM} = \mathbb{V}_L^{U\dagger} \mathbb{V}_L^D$, obtaining:

$$\mathbb{V}_{CKM} = \begin{pmatrix} \cos(\theta_{ds} - \theta_{uc}) & \sin(\theta_{ds} - \theta_{uc}) & r_U^+ \\ -\sin(\theta_{ds} - \theta_{uc}) & \cos(\theta_{ds} - \theta_{uc}) & r_2^{U+} \\ -r_D^+ & -r_D^- & 1 \end{pmatrix} \quad (104)$$

$$\equiv \begin{pmatrix} 1 - \frac{\lambda^2}{2} & \lambda & A\lambda^3(\rho - i\eta) \\ -\lambda & 1 - \frac{\lambda^2}{2} & A\lambda^2 \\ A\lambda^3(1 - \rho - i\eta) & -A\lambda^2 & 1 \end{pmatrix}, \quad (105)$$

where we have used the Wolfenstein parametrization and the parameters $r_{U,D}^\pm$ are defined by the following parameter rotation:

$$\begin{pmatrix} r_U^+ \\ r_U^- \end{pmatrix} = \begin{pmatrix} c_{uc} & -s_{uc} \\ s_{uc} & c_{ud} \end{pmatrix} \begin{pmatrix} r_1^D - r_1^U \\ r_2^D - r_2^U \end{pmatrix}, \quad \begin{pmatrix} r_D^+ \\ r_D^- \end{pmatrix} = \begin{pmatrix} c_{ds} & -s_{ds} \\ s_{ds} & c_{ds} \end{pmatrix} \begin{pmatrix} r_1^D - r_1^U \\ r_2^D - r_2^U \end{pmatrix}. \quad (106)$$

Since the Wolfenstein parametrization comes from an small angle expansion in the CKM matrix, we can approximate $\sin(\theta_{ds} - \theta_{uc}) \approx \theta_{ds} - \theta_{uc}$. Then, by comparing Eqs. (104) and (105) we see that rotation angles satisfy the constraint:

$$\theta_{ds} - \theta_{uc} \approx \lambda. \quad (107)$$

Due to the elevated number of free parameters in the quark sector, a parameter fitting can easily satisfy such constraint being also in agreement with quark masses. Besides, it implies that the dependence on the B meson anomaly relative branching fraction on θ_{ds} is identical as in figure 6 but shifted to the left $\lambda = 0.22650$ radians [29].

Furthermore, in order to improve the analysis, we perform a χ^2 fit with one degree of freedom according to [36]:

$$\chi^2 = \sum_i^3 \left(\frac{y_i - \mu_i}{\sigma_i} \right)^2 \quad (108)$$

where $y_i = \{R_K, R_{K^*}, \mathcal{B}[B_s \rightarrow \mu^+ \mu^-]\}$ represents the measured values and $\mu_i = \{R_K^{exp}, R_{K^*}^{exp}, \mathcal{B}[B_s \rightarrow \mu^+ \mu^-]_{exp}\}$ the experimental measurement with standard deviation $\sigma_i = \{\sigma_{R_K}, \sigma_{R_{K^*}}, \sigma_{\mathcal{B}_{B_s}}\}$. In particular, since the experimental values have asymmetrical errors, the mean value was taken. In general, the χ^2 fit impose restrictions on v_χ and θ_{uc} if we require $\chi^2 \leq \chi_{min}^2 + \chi_{CL}^2$, where it was found that $\chi_{min}^2 = 2.02$ and a 95% C.L. is chosen, corresponding to $\chi_{CL}^2 = 3.841$. We present in figure 8 the region in the (θ_{uc}, v_χ) plane compatible with such fit. In order to improve the speed of the numerical routine, the predictions for R_K and $\mathcal{B}[B_s \rightarrow \mu^+ \mu^-]$ were calculated using the analytic expressions shown in Eqs. (99) and (101) while the R_{K^*} is left for the flavio package. As a result, we see that the v_χ upper bound is raised to $v_\chi \leq 8.4$ TeV while all values for θ_{uc} are allowed, being in agreement with the results of figures 6, 7a and 7b. Besides, from Eq. (23) we get an increased Z' mass upper bound of 9.9 TeV.

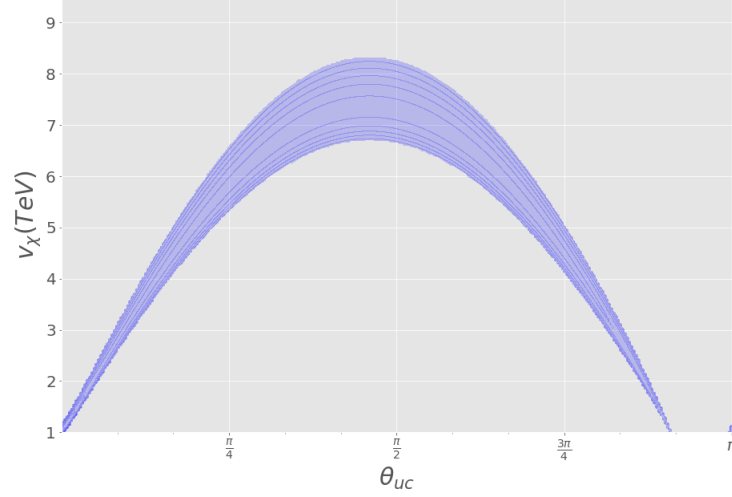


FIG. 8: Parameter region compatible with the observables R_K , R_{K^*} and $\mathcal{B}[B_s \rightarrow \mu^+ \mu^-]$ according to the χ^2 fit at 95% C.L.

VIII. MUON $g - 2$ ANOMALY

Since the model considers the existence of several new particles such as charged scalars and heavy Majorana neutrinos, their contributions to muon $g - 2$ can be considered as well. The different one-loop diagrams that might contribute are shown in figure 9.

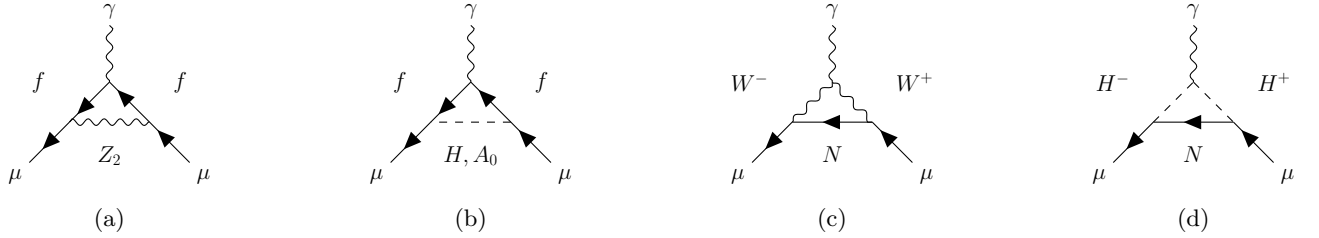


FIG. 9: Contribution to muon $g - 2$ from the interaction to Z' neutral gauge boson (a), (pseudo)scalars (b), charged W^+ gauge boson with exotic neutrinos (c) and charged scalars with neutrinos (d).

Thus, we need to consider neutrino interactions besides the considered in Eq. (25). The most general interaction Lagrangian involving neutral leptons is:

$$\mathcal{L}_{NL} = h_{2p}^{\nu w} \bar{\ell}_L^p \tilde{\phi}_2 \nu_R^w + h_{\chi q}^{\nu j} \bar{\nu}_R^w \chi^c N_R^j + \frac{1}{2} \bar{N}_R^i M_N^{ij} N_R^j, \quad (109)$$

where $p = e, \mu$ labels the lepton doublets, $w = e, \mu, \tau$ labels right-handed neutrinos and $i, j = e, \mu, \tau$ labels the Majorana neutrinos (see appendix A). Such Lagrangian is responsible of neutrino mass generation via inverse seesaw mechanism as shown in [37] and is able to reproduce the PMNS matrix as shown in [38]. In order to explore the general behavior of the model, we consider a benchmark scenario able to reproduce neutrino masses and PMNS matrix, identified by:

$$\begin{aligned} r_1 &= 3.5 \times 10^{-3}, & r_2 &= 1.08 \times 10^{-3}, \\ h_{2e}^{\nu e} &= 4.08 e^{-0.129i}, & h_{2\mu}^{\nu e} &= -2.28, \\ h_{2e}^{\nu \mu} &= 3.38 e^{0.216i}, & h_{2\mu}^{\nu \mu} &= 0.48, \\ h_{2e}^{\nu \tau} &= 4.70 e^{0.0103i}, & h_{2\mu}^{\nu \tau} &= 1.80, \\ \theta_{e\mu} &= 0.997. \end{aligned} \quad (110)$$

Besides, we consider the case where exotic neutrinos have nearly degenerate masses, $m_{\mathcal{N}_i} \approx m_{\mathcal{N}_j}$ for $i, j = 1, \dots, 6$, so their masses are given by the single mass parameters $m_{\mathcal{N}}$. Additionally, the lepton couplings q_{11} and q_{22} introduced in Eq. (25) have a negligible effect on lepton phenomenology. On the one hand, it has a negligible effect on charged lepton masses as they only appear in a suppressed term for the electron mass in Eq. (35). On the other hand, its effect on the PMNS matrix is given by the charged lepton rotation, where q_{11} and q_{12} are involved in the seesaw decoupling of the exotic E lepton and suppressed by m_E . Thus, q_{11} and q_{12} are given random values between 1 and 10, specifically $q_{11} = 5.957$ and $q_{12} = 7.373$. Finally, muon $g - 2$ contributions due to new physics effects are given in [39].

A. Flavor change mediated by Z_2^μ

First, neutral gauge bosons induce flavor changing neutral currents. Such an interaction produces a contribution to muon $g - 2$ at one-loop level according to figure 9a. The interaction terms between muon, E and Z_2 can be obtained easily from Eqs. (82) and (86) by writing the appropriate rotation matrix entries. It can be written as:

$$\begin{aligned} \mathcal{L} = & ig\bar{E}\not{Z}_2[(J_\tau^{L2} - J_{s'}^{L2})(\mathbb{V}_L^{E\dagger})^{E\tau}(\mathbb{V}_L^E)^{\tau\mu} + (J_E^{L2} - J_{s'}^{L2})(\mathbb{V}_L^{E\dagger})^{EE}(\mathbb{V}_L^E)^{E\mu})P_L \\ & + ((J_\mu^{R2} - J_p^{R2})(\mathbb{V}_R^{E\dagger})^{E\mu}(\mathbb{V}_R^E)^{\mu\mu} + (J_E^{R2} - J_p^{R2})(\mathbb{V}_R^{E\dagger})^{EE}(\mathbb{V}_R^E)^{E\mu})P_R]\mu. \end{aligned} \quad (111)$$

Rotation matrices indicate that $(\mathbb{V}_R^E)^{\mu\mu} = 1$, but $(\mathbb{V}_R^E)^{E\mu} \propto m_E^{-2}$, so we can neglect all the right-handed couplings. Furthermore, in the left-lepton rotation matrices we have $(\mathbb{V}_L^E)^{EE} = 1$ and $(\mathbb{V}_L^E)^{E\tau} = 0$, so we keep only the second line which is of the order $\mathcal{O}(m_E^{-1})$, resulting in:

$$\begin{aligned} \mathcal{L} = & ig\bar{E}\not{Z}_2[(J_E^{L2} - J_{s'}^{L2})(\mathbb{V}_L^{E\dagger})^{EE}(\mathbb{V}_L^E)^{E\mu})P_L]\mu + \text{H.C.} \\ = & ig\bar{E}\not{Z}_2\left[\left(\frac{s_Z}{2c_W} + \frac{g_X}{g}c_Z\right)(\mathbb{V}_L^{E\dagger})^{EE}(\mathbb{V}_L^E)^{E\mu})P_L\right]\mu + \text{H.C.} \\ \approx & -i\frac{v_1(s_{e\mu}q_{11} + c_{e\mu}q_{12})}{\sqrt{2}m_E}\bar{E}\left(\frac{g}{2c_W}s_Z + g_X\right)\not{Z}_2P_L\mu + \mathcal{O}\left(\frac{1}{m_E^2}\right) + \text{H.C.} \end{aligned} \quad (112)$$

The general expression for the muon $g - 2$ due to a mediating neutral gauge boson can be found in [39], which reads:

$$\Delta a_\mu^{Z_2} = \frac{1}{8\pi^2} \frac{m_\mu^2}{M_{Z_2}^2} \int_0^1 dx \frac{g_v^2 P_v(x) + g_a^2 P_a(x)}{(1-x)(1-\lambda^2 x) + \epsilon^2 \lambda^2 x}, \quad (113)$$

where

$$\begin{aligned} P_v(x) &= 2x(1-x)(x-2(1-\epsilon)) + \lambda^2(1-\epsilon)^2 x^2(1+\epsilon-x), \\ P_a(x) &= 2x(1-x)(x-2(1+\epsilon)) + \lambda^2(1+\epsilon)^2 x^2(1-\epsilon-x), \end{aligned} \quad (114)$$

$\epsilon = m_E/m_\mu$, $\lambda = m_\mu/M_{Z_2}$, and g_v and g_a are the vector and axial couplings respectively which in this case obey $g_v = -g_a \equiv g_{Z_2}$ defined as:

$$g_{Z_2} = -\frac{v_1(s_{e\mu}q_{11} + c_{e\mu}q_{12})}{2\sqrt{2}m_E} \left(\frac{g}{c_W}s_Z + 2g_X \right) \quad (115)$$

$$\approx -\frac{v_1 g_X (s_{e\mu}q_{11} + c_{e\mu}q_{12})}{\sqrt{2}m_E}. \quad (116)$$

Then, $\Delta a_\mu^{Z_2}$ can be written as:

$$\Delta a_\mu^{Z_2} = \frac{9}{4\pi^2} \frac{m_\mu^2}{v_\chi^2} \left(\frac{v_1(s_{e\mu}q_{11} + c_{e\mu}q_{12})}{\sqrt{2}m_E} \right)^2 \int_0^1 dx \frac{2x(1-x)(x-2) + \lambda^2 x^2(1-x - \epsilon^2(1+x))}{(1-x)(1-\lambda^2 x) + \epsilon^2 \lambda^2 x}. \quad (117)$$

After numerical integration, the muon $g - 2$ contribution as a function of m_E and m_{Z_2} is shown in figure 10 for $v_\chi = 15$ TeV. Since its contribution is negative, the absolute value is shown so it can be logarithmically scaled,

meaning that it cannot explain the anomaly by itself. Additionally, it can be seen that $\Delta a_\mu^{Z_2}$ is not sensitive to the Z_2 gauge boson mass, so from now on we can set a mass of $m_{Z_2} = 15$ TeV without affecting the results.

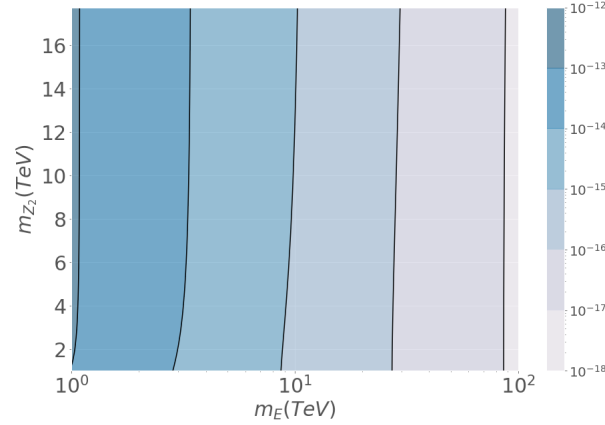


FIG. 10: Contours of the absolute value $|\Delta a_\mu^{Z_2}|$ of muon $g - 2$ contribution due to a Z_2 gauge boson and an exotic lepton E in the inner loop as a function of their masses for $v_1 = 246.218$ GeV, $v_\chi = 15$ TeV.

B. H and A^0 mediated flavor change

The contributions due to scalars and pseudoscalars are shown in figure 9b. By rotating to mass eigenstates in the Lagrangian in Eq. (25), we obtain the interaction among muon, scalars and the exotic lepton E , which at order $\mathcal{O}(m_E^{-1})$, reads:

$$-\mathcal{L}_{\mu\phi E} = -\frac{m_\mu t_\beta s_\beta}{\sqrt{2}m_E}(s_{e\mu}q_{11} + c_{e\mu}q_{12})\bar{E}_L\phi\mu_R + \frac{c_\beta}{\sqrt{2}}(s_{e\mu}q_{11} + c_{e\mu}q_{12})\bar{E}_R\phi\mu_L, \quad (118)$$

where $\phi = (H, iA^0)$ and using the approximations $c_{13} \approx c_\gamma \approx 1$. Then, the contribution to muon $g - 2$ can be written as:

$$\Delta a_\mu^{H,A^0} = \frac{1}{8\pi^2} \frac{m_\mu^2}{M_\phi^2} \int_0^1 dx \frac{g_s^2 P_s(x) + g_p^2 P_p(x)}{(1-x)(1-\lambda^2 x) + \epsilon^2 \lambda^2 x}, \quad (119)$$

with

$$P_s(x) = x^2(1 + \epsilon - x), \quad P_p(x) = x^2(1 - \epsilon - x), \quad (120)$$

$$\epsilon = \frac{m_E}{m_\mu}, \quad \lambda = \frac{m_\mu}{m_\phi}, \quad (121)$$

and g_s and g_p as the scalar and pseudoscalar couplings. Numerical integration shows that this contribution is negative and shows a similar behavior like the Z_2 contributions which showed big $|\Delta a_\mu|$ values for small TeV masses. The total contribution due to scalars, pseudoscalars and Z_2 is shown in figure 11, where $m_H \approx m_{A^0}$ according to section III. We see that in general there is an important suppression due to m_E which can be seen from the couplings depending on m_E^{-1} , while in the case of the left-handed couplings of scalars, it is suppressed by $c_\beta \approx 1/246$. The flavor changing neutral interactions provide negligible contributions to muon $g - 2$.

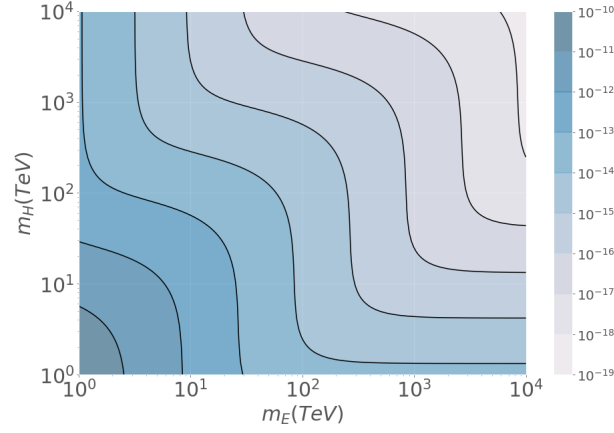


FIG. 11: Contours of the absolute value added contributions $|\Delta a_\mu^{Z_2} + \Delta a_\mu^H + \Delta a_\mu^{A^0}|$ to muon $g - 2$ due to diagrams in figure 9a and 9b as a function of the charged scalar mass and the exotic lepton mass.

C. Charged W^+ boson and exotic neutrinos

From the electroweak charged current, we can obtain an interaction involving the muon, W^+ and exotic neutrinos \mathcal{N} . The interaction in terms of mass eigenstates can be written as:

$$\mathcal{L}_{W\mathcal{N}\mu} = -\bar{\mathcal{N}}^j W_\mu^+ \frac{g_{v2}\gamma^\mu}{4m_{\mathcal{N}}} [s_{\theta_{e\mu}} h_{2e,\mu}(j) + c_{\theta_{e\mu}} h_{2\mu}(j)] P_L \mu, \quad (122)$$

where the $h_{2e,\mu}(j)$ couplings are defined as:

$$\begin{aligned} h_{2e,\mu}(1) &= -ih_{2e,\mu}^{\nu e}, & h_{2e,\mu}(4) &= h_{2e,\mu}^{\nu e}, \\ h_{2e,\mu}(2) &= -ih_{2e,\mu}^{\nu \mu}, & h_{2e,\mu}(5) &= h_{2e,\mu}^{\nu \mu}, \\ h_{2e,\mu}(3) &= -ih_{2e,\mu}^{\nu \tau}, & h_{2e,\mu}(6) &= h_{2e,\mu}^{\nu \tau}, \end{aligned} \quad (123)$$

and $j = 1, \dots, 6$. Their contribution to muon $g - 2$ is according to the loop diagram shown in figure 9c which can be written as:

$$\Delta a_\mu^{W\mathcal{N}_j} = \frac{1}{8\pi^2} \frac{m_\mu^2}{M_{H^+}^2} \int_0^1 dx \frac{g_s^2 P_s(x) + g_p^2 P_p(x)}{(1-x)(1-\lambda^2 x) + \epsilon^2 \lambda^2 x}, \quad (124)$$

where

$$\begin{aligned} P_s(x) &= 2x^2(1+x-2\epsilon) + \lambda^2(1-\epsilon)^2 x(1-x)(x+\epsilon), \\ P_p(x) &= 2x^2(1+x+2\epsilon) + \lambda^2(1+\epsilon)^2 x(1-x)(x-\epsilon), \end{aligned} \quad (125)$$

$\epsilon = \frac{m_{\mathcal{N}}}{m_\mu}$ and $\lambda = \frac{m_\mu}{m_{W^+}}$. This contribution is positive and highly sensitive to neutrino Yukawa couplings $h_{2e}^{\nu q}$ and $h_{2\mu}^{\nu q}$. Massive neutrinos have a mass around the 10^{-3} eV scale, whose smallness can be justified by the overall factor $\frac{\mu_N v_2^2}{h_{N\chi 1}^2 v_\chi^2}$, as shown in the appendix A. In this way, we see that the smaller the factor is, the bigger Yukawa couplings are. Such requirement translate in an estimate for the μ_N parameter given by:

$$\begin{aligned} \frac{\mu_N v_2^2}{h_{N\chi 1}^2 v_\chi^2} &= \frac{\mu_N v_2^2}{2m_{\mathcal{N}}^2} \sim 10^{-3} \text{ eV} \\ \mu_N &\sim 2m_{\mathcal{N}}^2 \times 10^{-3} \text{ eV}, \end{aligned} \quad (126)$$

for $v_2 = 1$ GeV as stated above. The plot in figure 12 shows the behavior of the $g - 2$ contribution as a function of the exotic neutrino masses for different values of μ_N .

Since a lower bound for heavy Majorana neutrinos of 1.2 TeV was reported in [40], we can obtain an upper bound on μ_N according to such mass and the muon $g - 2$ at 90% C.L. given by $\mu_N = 0.45m_{\mathcal{N}}^2 \times 10^{-3}$ eV (orange curve). Nevertheless, for smaller values of μ_N we obtain larger contributions for relative small exotic neutrino masses.

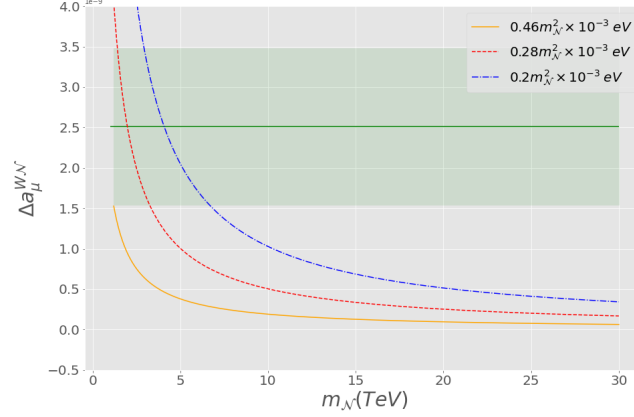


FIG. 12: Added contributions $\sum_{i=1}^6 \Delta a_{\mu}^{W, \mathcal{N}_i} \equiv \Delta a_{\mu}^{W, \mathcal{N}}$ to muon $g - 2$ due to a W^+ and the exotic neutrinos with nearly degenerate masses as a function of $m_{\mathcal{N}}$ for different values of μ_N . The green region represents the experimental value at 90% C.L..

D. Charged scalars and exotic neutrinos

An important contribution comes by considering charged scalars H^{\pm} and exotic neutrinos \mathcal{N}_j as shown in figure 9d. By rotating to mass eigenstates, we obtain from the Lagrangian in Eq. (109) the relevant interactions among heavy neutrinos, charged scalars and the muon. It reads:

$$\mathcal{L}_{\mathcal{N}H^{\pm}\mu} = \frac{v_1 q_{11}}{\sqrt{2}m_E} s_{\beta} h_{2e}^*(q) (R_{\nu}^{\dagger})_{kq} \bar{\nu}_R^k H^+ E_L + \frac{v_1 q_{12}}{\sqrt{2}m_E} s_{\beta} h_{2\mu}^*(q) (R_{\nu}^{\dagger})_{kq} \bar{\nu}_R^k H^+ E_L, \quad (127)$$

where $k = 4, \dots, 9$ is used only for exotic neutrino mass eigenstates, $q = 4, 5, 6$ and $h_{2e,\mu}(q)$ is defined in Eq. (123). In general we can neglect the contributions coming from Eq. (25) because the neutrino rotation matrix provides an important suppression. The muon $g - 2$ contribution can be written as:

$$\Delta a_{\mu}^{H^{\pm}\mathcal{N}_j} = \frac{1}{8\pi^2} \frac{m_{\mu}^2}{M_{H^+}^2} \int_0^1 dx \frac{g_s^2 P_s(x) + g_p^2 P_p(x)}{(1-x)(1-\lambda^2 x) + \epsilon^2 \lambda^2 x}, \quad (128)$$

where

$$P_s(x) = -x(1-x)(x+\epsilon), \quad P_p(x) = -x(1-x)(x-\epsilon), \quad (129)$$

$$\epsilon = \frac{m_{\mathcal{N}}}{m_{\mu}}, \quad \lambda = \frac{m_{\mu}}{m_{H^+}}. \quad (130)$$

Since $m_{H^{\pm}} \approx m_H$ we can compare this contribution to the neutral scalar case by considering nearly degenerate exotic neutrinos as well, so we can add the contributions due to all six neutrinos, which gives the absolute value for the muon $g - 2$ shown in figure 13. Despite the contribution is also negative, it provides bigger values than the neutral scalar contributions, which all together counteract the W^+ gauge boson contribution to fit the anomaly. Besides, it was considered for this graph them the exotic neutrino mass at 1.2 TeV and obtain the maximum negative contribution in order to compensate the positive contributions arisen from the W^{\pm} loop.

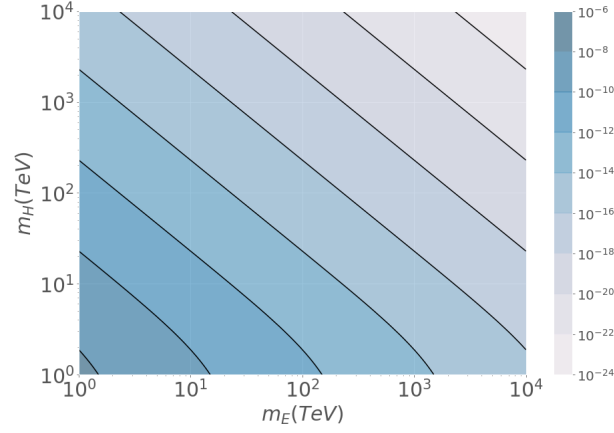


FIG. 13: Contours of the absolute value added contributions $|\sum_{i=1}^6 \Delta a_\mu^{H^\pm \mathcal{N}_j}| \equiv |\Delta a_\mu^{H^\pm \mathcal{N}}|$ to muon $g - 2$ due to the six nearly degenerate neutrinos as a function of the charged scalar mass $m_{H^\pm} \approx m_H$ and the exotic lepton mass for $m_{\mathcal{N}} = 1.2$ TeV.

E. Total $g - 2$ prediction

We saw that the interaction with W^+ bosons provides a positive contribution to muon $g - 2$ while in the case of neutral and charged scalars, the contributions are negative with big values for small masses in the TeV scale i.e. $1 - 2$ TeV. Now, we add all contributions shown in figure 9 to find the allowed region in parameter space that fits the anomaly. In particular, we consider $\mu_{\mathcal{N}} = 0.2 m_{\mathcal{N}}^2 \times 10^{-3}$ eV, nearly degenerate exotic neutrino masses and the parameter choice shown in Eq. (110). In figure 14 we display the allowed regions compatible with the muon $g - 2$ for three different values of $m_{\mathcal{N}}$.

First, the lower mass bound for exotic neutrino is taken at 1.2 TeV (blue region), according to the ATLAS experiment [40]. In this case, the positive contribution due to diagram 9c is bigger than the experimental value, so small m_E and m_H masses are required to generate a negative contribution of the same order that counteracts its value. Furthermore, from figure 12 we see that there is an upper bound for the exotic neutrino mass of 6.7 TeV at 90% C.L. from muon $g - 2$, where the anomaly can be explained entirely by the interaction with W bosons (diagram 9c) and contributions due to heavy scalars must be small enough to not decrease the total $g - 2$ out of the 90 % C.L. interval. For instance, when the heavy neutrino takes a mass value close to the upper limit of 6.5 TeV, represented by the pink region in figure 14, a lower mass bound for m_E and m_H is represented by the boundary of the region, whose values are bigger than the bounds set for intermediate values of $m_{\mathcal{N}}$, such as $m_{\mathcal{N}} = 5$ TeV in the purple region which lead to bigger negative contributions. Last but not least, it is worth to notice that the total $g - 2$ implies masses of the same order, so in spite of the v_χ dependence of m_E , $m_{\mathcal{N}}$ and m_H , they can be justified by Yukawa couplings of order 1.

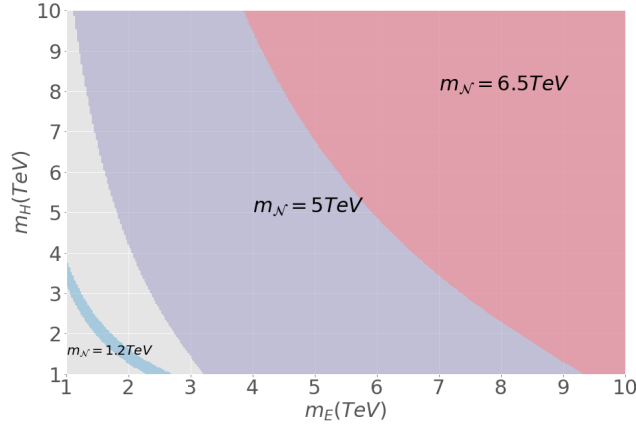


FIG. 14: Allowed masses for the exotic lepton E and heavy scalars compatible with muon $g - 2$ at 90 % C.L. for different exotic neutrino masses: $m_{\mathcal{N}} = 1.2$ TeV in blue, $m_{\mathcal{N}} = 5$ TeV in purple and $m_{\mathcal{N}} = 12$ TeV in pink. The total $g - 2$ contribution has been calculated as $|\Delta a_{\mu}^{Tot}| = |\Delta a_{\mu}^{Z_2} + \Delta a_{\mu}^{W\mathcal{N}} + \Delta a_{\mu}^{H^{\pm}\mathcal{N}} + \Delta a_{\mu}^H + \Delta a_{\mu}^{A^0}|$.

IX. CONCLUSIONS

The non-universal extension $\mathcal{G}_{SM} \otimes U(1)_X$ is consistent to the absence of heavy fermion masses thanks to its dependence on a particular VEV. Thereby, top quark mass is justified by v_1 while the bottom quark, the τ and muon lepton masses have smaller masses in comparison due to their dependence on v_2 . Moreover, exotic particle masses are justified by the scalar singlet VEV v_{χ} which is expected to lie at the TeV scale while the lightest fermions such as the electron and the up, down and strange quarks are massless at tree-level, but their masses are explained by considering the effects of non-renormalizable operators allowed by the $U(1)_X \otimes \mathbb{Z}_2$ symmetry up to dimension 7, which in general fill all zeros in mass matrices. General expressions for mass eigenvalues and rotation matrices are obtained as well as upper bounds for the effective operators energy scale Λ which is required to be $\Lambda \leq 4.7v_{\chi}$ in order to explain all light masses simultaneously.

Regarding the flavor changing neutral interactions among quarks were obtained as well as the non-universal interaction among neutral gauge bosons, quarks and leptons, to provide an explanation consistent to the observed B meson anomaly. The interaction with the Z_1^{μ} gauge boson mass eigenstate is discarded since it is approximately equal to the SM Z^{μ} gauge boson, while the interactions with Z_2^{μ} generate additional contributions to the relevant Wilson coefficients. Consequently, the relative branching fraction is not sensitive to g_X variations but it sets the upper bounds $v_{\chi} \leq 8.4$ TeV and $m_{Z_2} \leq 9.9$ TeV according to the χ^2 fit and if we assume the new interaction to be valid in the perturbative regime. Besides, the relative branching fraction is parametrized by θ_{uc} , providing allowed regions for the angles depending on the value of v_{χ} employed.

Finally, muon $g - 2$ contributions were calculated by considering the interactions of heavy scalars, both neutral and charged, to the exotic lepton E and exotic neutrinos which resulted in negative contributions. However, the interaction between the SM W^+ gauge boson to exotic neutrinos provides the only positive contribution which can reach the experimental value if Yukawa couplings for neutral leptons are greater than 4.5. We consider a benchmark scenario where exotic neutrino masses are nearly degenerate and Yukawa couplings range from 9 to 50. It was shown that if exotic neutrino masses are of a few TeV, heavy scalars and the exotic lepton have masses of the same order, but if the exotic neutrino masses are big enough to be in the limit on the 90 % confidence level, heavy scalars and the exotic lepton are allowed to have arbitrary large masses, because their contributions become negligible small. All in all, the non-universal extension has proven to be compatible with SM phenomenology while it also explains the reported anomalies.

Appendix A: Neutrino masses and rotation matrix

From Eq. (109) we write the 9×9 neutrino mass matrix in the basis $(\nu_L^{e,\mu,\tau}, (\nu_R^{e,\mu,\tau})^C, (N_R^{e,\mu,\tau})^C)$ as:

$$\mathcal{M}_\nu = \begin{pmatrix} 0 & m_D^T & 0 \\ m_D & 0 & M_D^T \\ 0 & M_D & M_M \end{pmatrix}, \quad (\text{A1})$$

where the block matrices are defined as:

$$m_D^T = \frac{v_2}{\sqrt{2}} \begin{pmatrix} h_{2e}^{\nu e} & h_{2e}^{\nu\mu} & h_{2e}^{\nu\tau} \\ h_{2\mu}^{\nu e} & h_{2\mu}^{\nu\mu} & h_{2\mu}^{\nu\tau} \\ 0 & 0 & 0 \end{pmatrix}, \quad (M_D)^{ij} = \frac{v_\chi}{\sqrt{2}} h_{\chi i}^{\nu j}, \quad (M_M)_{ij} = \frac{1}{2} M_N^{ij}. \quad (\text{A2})$$

Neutrino masses are generated via inverse seesaw mechanism by assuming the hierarchy $M_M \ll m_D \ll M_D$. Block diagonalization is achieved by the rotation matrix \mathbb{V}_{SS} given by:

$$\mathbb{V}_{SS} \mathcal{M}_\nu \mathbb{V}_{SS}^\dagger \approx \begin{pmatrix} m_{\text{light}} & 0 \\ 0 & m_{\text{heavy}} \end{pmatrix}, \quad \mathbb{V}_{SS} = \begin{pmatrix} I & -\Theta_\nu \\ \Theta_\nu^\dagger & I \end{pmatrix}, \quad \Theta_\nu = \begin{pmatrix} m_D^\dagger & 0 \end{pmatrix} \begin{pmatrix} 0 & M_D^T \\ M_D & M_M \end{pmatrix}^{-1*}, \quad (\text{A3})$$

where $m_{\text{light}} = m_D^T (M_D^T)^{-1} M_M (M_D)^{-1} m_D$ is the 3×3 mass matrix containing the active neutrinos and m_{heavy} contains the six heavy Majorana neutrino mass eigenstates, which reads:

$$m_{\text{heavy}} \approx \begin{pmatrix} 0 & M_D^T \\ M_D & M_M \end{pmatrix}. \quad (\text{A4})$$

For simplicity, let's consider the case of M_D being diagonal and M_M proportional to the identity.

$$M_D = \frac{v_\chi}{\sqrt{2}} \begin{pmatrix} h_{N\chi e} & 0 & 0 \\ 0 & h_{N\chi\mu} & 0 \\ 0 & 0 & h_{N\chi\tau} \end{pmatrix}, \quad M_M = \mu_N \mathbb{I}_{3 \times 3}. \quad (\text{A5})$$

Thus, light neutrino mass matrix takes the form:

$$m_{\text{light}} = \frac{\mu_N v_2^2}{h_{N\chi e}^2 v_\chi^2} \begin{pmatrix} (h_{2e}^{\nu e})^2 + (h_{2\mu}^{\nu e})^2 \rho^2 & h_{2e}^{\nu e} h_{2e}^{\nu\mu} + h_{2\mu}^{\nu e} h_{2\mu}^{\nu\mu} \rho^2 & h_{2e}^{\nu e} h_{2e}^{\nu\tau} + h_{2\mu}^{\nu e} h_{2\mu}^{\nu\tau} \rho^2 \\ h_{2e}^{\nu e} h_{2e}^{\nu\mu} + h_{2\mu}^{\nu e} h_{2\mu}^{\nu\mu} \rho^2 & (h_{2e}^{\nu\mu})^2 + (h_{2\mu}^{\nu\mu})^2 \rho^2 & h_{2e}^{\nu\mu} h_{2e}^{\nu\tau} + h_{2\mu}^{\nu\mu} h_{2\mu}^{\nu\tau} \rho^2 \\ h_{2e}^{\nu e} h_{2e}^{\nu\tau} + h_{2\mu}^{\nu e} h_{2\mu}^{\nu\tau} \rho^2 & h_{2e}^{\nu\mu} h_{2e}^{\nu\tau} + h_{2\mu}^{\nu\mu} h_{2\mu}^{\nu\tau} \rho^2 & (h_{2e}^{\nu\tau})^2 + (h_{2\mu}^{\nu\tau})^2 \rho^2 \end{pmatrix}, \quad (\text{A6})$$

where $\rho = h_{N\chi e}/h_{N\chi\mu}$. m_{light} has rank 2 so it contains a massless neutrino which is still allowed because experiments provide squared mass differences. Besides, we see that there is an overall factor which we assume to be the responsible of providing the mass energy scale. However, exotic neutrinos mass eigenstates, \mathcal{N}^k , $k = 1, \dots, 6$, can be obtained easily from Eq. (A5) being the mass eigenvalues given by:

$$m_{\mathcal{N}^1} = \frac{1}{2}(\mu_N - \sqrt{\mu_N^2 + 2h_{N\chi e}^2 v_\chi^2}), \quad m_{\mathcal{N}^4} = \frac{1}{2}(\mu_N + \sqrt{\mu_N^2 + 2h_{N\chi e}^2 v_\chi^2}), \quad (\text{A7})$$

$$m_{\mathcal{N}^2} = \frac{1}{2}(\mu_N - \sqrt{\mu_N^2 + 2h_{N\chi\mu}^2 v_\chi^2}), \quad m_{\mathcal{N}^5} = \frac{1}{2}(\mu_N + \sqrt{\mu_N^2 + 2h_{N\chi\mu}^2 v_\chi^2}), \quad (\text{A8})$$

$$m_{\mathcal{N}^3} = \frac{1}{2}(\mu_N - \sqrt{\mu_N^2 + 2h_{N\chi\tau}^2 v_\chi^2}), \quad m_{\mathcal{N}^6} = \frac{1}{2}(\mu_N + \sqrt{\mu_N^2 + 2h_{N\chi\tau}^2 v_\chi^2}). \quad (\text{A9})$$

Finally, the diagonal mass eigenstates are given by $\mathcal{M}_\nu^{\text{diag}} = \mathcal{R} \mathcal{M}_\nu \mathcal{R}^\dagger$ where the rotation matrix is given by:

$$\mathcal{R} \approx \left(\begin{array}{c|cc} V^\nu & 0 & V^\nu m_D^\dagger M_D^{-1*} \\ \hline -\frac{i}{\sqrt{2}} M_D^{-1T} m_D & i \frac{1}{\sqrt{2}} \mathbb{I} & -i \frac{1}{\sqrt{2}} \mathbb{I} \\ \frac{1}{\sqrt{2}} M_D^{-1T} m_D & \frac{1}{\sqrt{2}} \mathbb{I} & \frac{1}{\sqrt{2}} \mathbb{I} \end{array} \right), \quad (\text{A10})$$

where V^ν is the rotation matrix for active neutrinos. Since the term μ_N is very small ($\mu_N \sim 2m_N^2 \times 10^{-12}$ GeV) in comparison to v_χ , it can be neglected making the first three exotic neutrino mass eigenvalues to be negative. which makes exotic neutrinos mass eigenstates nearly degenerate, so the i factor in the second row arises to make all eigenvalues positive.

-
- [1] P. Minkowski, Physics Letters B **67**, 421 (1977); M. Gell-Mann, P. Ramond, and R. Slansky, Amsterdam: North-Holland) p **315**, 687 (1979); T. Yanagida, KEK Report No. 79-18 **95** (1979); E. Molinaro, Journal of Physics: Conference Series **447**, 012052 (2013); T. Yanagida and J. Tsukuba, Phys. Rev. Lett **44**, 912 (1980); J. Schechter and J. W. Valle, Physical Review D **25**, 774 (1982); **22**, 2227 (1980); A. G. Dias, C. d. S. Pires, P. R. da Silva, and A. Sampieri, **86**, 035007 (2012).
- [2] M. Misiak and M. Steinhauser, The European Physical Journal C **77**, 1 (2017).
- [3] G. Aad, B. Abbott, J. Abdallah, R. Aben, M. Abolins, O. AbouZeid, H. Abramowicz, H. Abreu, R. Abreu, Y. Abulaiti, *et al.*, Journal of High Energy Physics **2015**, 1 (2015).
- [4] B. e. a. Abi (Muon $g - 2$ Collaboration), Phys. Rev. Lett. **126**, 141801 (2021); G. W. Bennett, B. Bousquet, H. Brown, G. Bunce, R. Carey, P. Cushman, G. Danby, P. Debevec, M. Deile, H. Deng, *et al.*, Physical Review D **73**, 072003 (2006); T. Aoyama, N. Asmussen, M. Benayoun, J. Bijnens, T. Blum, M. Bruno, I. Caprini, C. C. Calame, M. Cè, G. Colangelo, *et al.*, Physics reports (2020); S. Borsanyi, Z. Fodor, J. Guenther, C. Hoelbling, S. Katz, L. Lellouch, T. Lippert, K. Miura, L. Parato, K. Szabo, *et al.*, Nature **593**, 51 (2021); H. Terazawa, Progress of Theoretical Physics **39**, 1326 (1968); Nonlinear Phenomena in Complex Systems **21**, 268 (2018).
- [5] A. Keshavarzi, in *EPJ Web of Conferences*, Vol. 212 (EDP Sciences, 2019) p. 05003; G. Bennett, B. Bousquet, H. Brown, G. Bunce, R. Carey, P. Cushman, G. Danby, P. Debevec, M. Deile, H. Deng, *et al.*, Physical Review Letters **89**, 101804 (2002).
- [6] R. Carey, K. Lynch, J. Miller, B. Roberts, W. Morse, Y. Semertzides, V. Druzhinin, B. Khazin, I. Koop, I. Logashenko, *et al.*, *The New (g-2) Experiment: A proposal to measure the muon anomalous magnetic moment to ± 0.14 ppm precision*, Tech. Rep. (Fermi National Accelerator Lab.(FNAL), Batavia, IL (United States), 2009).
- [7] M. Abe, S. Bae, G. Beer, G. Bunce, H. Choi, S. Choi, M. Chung, W. Da Silva, S. Eidelman, M. Finger, *et al.*, Progress of Theoretical and Experimental Physics **2019**, 053C02 (2019).
- [8] C. Kelso, H. Long, R. Martinez, and F. S. Queiroz, Physical Review D **90**, 113011 (2014).
- [9] P. Ferreira, B. Gonçalves, F. Joaquim, and M. Sher, arXiv preprint arXiv:2104.03367 (2021); A. Crivellin, N. Asmussen, M. Benayoun, *et al.*, Physics Reports , Epub (2020); G. Arcadi, Á. S. de Jesus, T. B. de Melo, F. S. Queiroz, and Y. S. Villamizar, arXiv preprint arXiv:2104.04456 (2021); P. Ferreira, B. Gonçalves, F. Joaquim, and M. Sher, arXiv preprint arXiv:2104.03367 (2021); R. Dermisek and A. Raval, Physical Review D **88**, 013017 (2013); R. Dermisek, K. Hermanek, and N. McGinnis, arXiv preprint arXiv:2103.05645 (2021); A. Crivellin, J. Heeck, and P. Stoffer, Physical review letters **116**, 081801 (2016); A. Crivellin, D. Müller, and C. Wiegand, Journal of High Energy Physics **2019**, 1 (2019); H.-X. Wang, L. Wang, and Y. Zhang, arXiv preprint arXiv:2104.03242 (2021).
- [10] A. Kamada, K. Kaneta, K. Yanagi, and H.-B. Yu, Journal of High Energy Physics **2018**, 1 (2018); A. Biswas, S. Choubey, and S. Khan, **2017**, 123 (2017).
- [11] S. Baek, Physics Letters B **756**, 1 (2016).
- [12] A. C. Hernández, S. King, H. Lee, and S. Rowley, Physical Review D **101**, 115016 (2020); A. Falkowski, S. F. King, E. Perdomo, and M. Pierre, Journal of High Energy Physics **2018**, 1 (2018); A. C. Hernández, S. Kovalenko, R. Pasechnik, and I. Schmidt, The European Physical Journal C **79**, 1 (2019); B. Allanach, F. S. Queiroz, A. Strumia, and S. Sun, Physical Review D **93**, 055045 (2016); S. Raby and A. Trautner, **97**, 095006 (2018); J. Kawamura, S. Raby, and A. Trautner, **100**, 055030 (2019); A. J. Buras, A. Crivellin, F. Kirk, C. A. Manzari, and M. Montull, arXiv preprint arXiv:2104.07680 (2021).
- [13] M. Endo, K. Hamaguchi, S. Iwamoto, and T. Yoshinaga, Journal of High Energy Physics **2014**, 123 (2014); M. Lindner, M. Platscher, and F. S. Queiroz, Physics Reports **731**, 1 (2018); M. A. Ajaib, I. Gogoladze, Q. Shafi, and C. S. Ün, Journal of High Energy Physics **2014**, 79 (2014); H. Davoudiasl, H.-S. Lee, and W. J. Marciano, Physical Review D **89**, 095006 (2014); V. Rantala, W. Shepherd, and S. Su, **84**, 035004 (2011); C. Kelso, P. Pinheiro, F. S. Queiroz, and W. Shepherd, The European Physical Journal C **74**, 1 (2014); N. A. Ky, H. N. Long, and D. Van Soa, Physics Letters B **486**, 140 (2000); C. d. S. Pires and P. R. da Silva, Physical Review D **64**, 117701 (2001); P. Agrawal, Z. Chacko, and C. B. Verhaaren, Journal of High Energy Physics **2014**, 1 (2014); M. Endo, K. Hamaguchi, T. Kitahara, and T. Yoshinaga, **2013**, 13 (2013); C. Majumdar, S. Patra, P. Pritimita, S. Senapati, and U. A. Yajnik, arXiv preprint arXiv:2004.14259 (2020); J. Ellis, M. A. Garcia, N. Nagata, D. V. Nanopoulos, and K. A. Olive, Journal of Cosmology and Astroparticle Physics **2020**, 035 (2020); C. Majumdar, S. Patra, P. Pritimita, S. Senapati, and U. A. Yajnik, arXiv preprint arXiv:2004.14259 (2020); W. Altmannshofer, C.-Y. Chen, P. B. Dev, and A. Soni, Physics Letters B **762**, 389 (2016); E. Megías, M. Quirós, and L. Salas, Journal of High Energy Physics **2017**, 16 (2017); M. Yamaguchi and W. Yin, Progress of Theoretical and Experimental Physics **2018**, 023B06 (2018); W. Yin and N. Yokozaki, Physics Letters B **762**, 72 (2016); M. Endo and W. Yin, Journal of High Energy Physics **2019**, 1 (2019); M. Bauer and M. Neubert, arXiv preprint arXiv:1511.01900 (2015); A. Crivellin, D. Mueller, and F. Saturnino, arXiv preprint arXiv:2008.02643 (2020); A. Crivellin and M. Hoferichter, arXiv preprint arXiv:1905.03789 (2019); arXiv preprint arXiv:2104.03202 (2021); E. Coluccio Leskow, A. Crivellin, D. Muller, *et al.*, Bulletin of the American Physical Society **63** (2018); A. Crivellin,

- D. Müller, and F. Saturnino, *Journal of High Energy Physics* **2020**, 020 (2020); W. Altmannshofer, M. Carena, and A. Crivellin, *Physical Review D* **94**, 095026 (2016); P. Arnan, A. Crivellin, M. Fedele, and F. Mescia, *Journal of High Energy Physics* **2019**, 1 (2019); H. Terazawa, *Progress of Theoretical Physics* **40**, 830 (1968); P. Athron, C. Balázs, D. H. Jacob, W. Kotlarski, D. Stöckinger, and H. Stöckinger-Kim, arXiv preprint arXiv:2104.03691 (2021).
- [14] R. Aaij, C. A. Beteta, T. Ackernley, B. Adeva, M. Adinolfi, H. Afsharnia, C. A. Aidala, S. Aiola, Z. Ajaltouni, S. Akar, *et al.*, arXiv preprint arXiv:2103.11769 (2021).
- [15] R. Aaij, B. Adeva, M. Adinolfi, Z. Ajaltouni, S. Akar, J. Albrecht, F. Alessio, M. Alexander, S. Ali, G. Alkhazov, *et al.*, *Journal of High Energy Physics* **2017** (2017).
- [16] W. Altmannshofer and P. Stangl, arXiv preprint arXiv:2103.13370 (2021).
- [17] M. Beneke, C. Bobeth, and R. Szafron, *Journal of High Energy Physics* **2019**, 1 (2019).
- [18] B. Capdevila, A. Crivellin, S. Descotes-Genon, J. Matias, and J. Virto, *Journal of High Energy Physics* **2018**, 1 (2018); W. Altmannshofer, P. Stangl, and D. M. Straub, *Physical Review D* **96**, 055008 (2017); L.-S. Geng, B. Grinstein, S. Jäger, J. M. Camalich, X.-L. Ren, and R.-X. Shi, **96**, 093006 (2017); M. Ciuchini, A. M. Coutinho, M. Fedele, E. Franco, A. Paul, L. Silvestrini, and M. Valli, *The European Physical Journal C* **77**, 1 (2017); A. K. Alok, B. Bhattacharya, A. Datta, D. Kumar, J. Kumar, and D. London, *Physical Review D* **96**, 095009 (2017); A. Celis, J. Fuentes-Martin, A. Vicente, and J. Virto, **96**, 035026 (2017); G. D'Amico, M. Nardecchia, P. Panci, F. Sannino, A. Strumia, R. Torre, and A. Urbano, *Journal of High Energy Physics* **2017**, 1 (2017); A. Crivellin, C. A. Manzari, M. Alguero, and J. Matias, arXiv preprint arXiv:2010.14504 (2020); L. Calibbi, A. Crivellin, F. Kirk, C. A. Manzari, and L. Vernazza, *Physical Review D* **101**, 095003 (2020); A. Crivellin, L. Hofer, J. Matias, U. Nierste, S. Pokorski, and J. Rosiek, **92**, 054013 (2015).
- [19] S. Descotes-Genon, J. Matias, and J. Virto, *Phys. Rev. D* **88**, 074002 (2013), arXiv:1307.5683 [hep-ph]; L. Bian, S.-M. Choi, Y.-J. Kang, and H. M. Lee, *Physical Review D* **96**, 075038 (2017); G. Hiller and M. Schmaltz, **90**, 054014 (2014); S. Descotes-Genon, T. Hurth, J. Matias, and J. Virto, *Journal of High Energy Physics* **2013**, 137 (2013); G. Bélanger, C. Delaunay, and S. Westhoff, *Physical Review D* **92**, 055021 (2015); W. Altmannshofer and I. Yavin, **92**, 075022 (2015); W. Altmannshofer, S. Gori, S. Profumo, and F. S. Queiroz, *Journal of High Energy Physics* **2016**, 1 (2016); P. Ko, T. Nomura, and H. Okada, arXiv preprint arXiv:1702.02699 (2017); J. M. Cline, J. M. Cornell, D. London, and R. Watanabe, *Physical Review D* **95**, 095015 (2017); J. F. Kamenik, Y. Soreq, and J. Zupan, **97**, 035002 (2018); S. Di Chiara, A. Fowlie, S. Fraser, C. Marzo, L. Marzola, M. Raidal, and C. Spethmann, *Nuclear Physics B* **923**, 245 (2017); R. Alonso, P. Cox, C. Han, and T. T. Yanagida, *Physical Review D* **96**, 071701 (2017); S. F. King, *Journal of High Energy Physics* **2017**, 1 (2017); A. Crivellin, G. D'Ambrosio, and J. Heeck, *Phys. Rev. Lett* **114**, 151801 (2015); P. Ko, T. Nomura, and H. Okada, *Physics Letters B* **772**, 547 (2017); D. Bhatia, S. Chakraborty, and A. Dighe, *Journal of High Energy Physics* **2017**, 117 (2017); R. Alonso, P. Cox, C. Han, and T. T. Yanagida, *Physics Letters B* **774**, 643 (2017); Y. Tang and Y.-L. Wu, arXiv preprint arXiv:1705.05643 (2017); S. M. Boucenna, A. Celis, J. Fuentes-Martin, A. Vicente, and J. Virto, *Physics Letters B* **760**, 214 (2016); **760**, 214 (2016); D. Das, C. Hati, G. Kumar, and N. Mahajan, *Physical Review D* **94**, 055034 (2016); P. T. Hutaurok, T. Nomura, H. Okada, and Y. Orikasa, **99**, 055041 (2019); E. Megías, M. Quiros, and L. Salas, *Journal of High Energy Physics* **2017**, 1 (2017); E. Megías, M. Quirós, and L. Salas, *Physical Review D* **96**, 075030 (2017).
- [20] H. Baer, V. Barger, and H. Serce, arXiv preprint arXiv:2104.07597 (2021); M. Endo, K. Hamaguchi, S. Iwamoto, and T. Kitahara, arXiv preprint arXiv:2104.03217 (2021); S. Baum, M. Carena, N. R. Shah, and C. E. Wagner, arXiv preprint arXiv:2104.03302 (2021); W. Altmannshofer, P. B. Dev, A. Soni, and Y. Sui, *Physical Review D* **102**, 015031 (2020).
- [21] S. Biswas, D. Chowdhury, S. Han, and S. J. Lee, *Journal of High Energy Physics* **2015**, 142 (2015); D. Das, C. Hati, G. Kumar, and N. Mahajan, *Physical Review D* **96**, 095033 (2017); M. Bauer and M. Neubert, *Phys. Rev. Lett* **116**, 141802 (2016); C.-H. Chen, T. Nomura, and H. Okada, arXiv preprint arXiv:1703.03251 (2017); G. Hiller and I. Nišandžić, *Physical Review D* **96**, 035003 (2017); Y. Cai, J. Gargalionis, M. A. Schmidt, and R. R. Volkas, *Journal of High Energy Physics* **2017**, 1 (2017); M. Blanke and A. Crivellin, *Physical review letters* **121**, 011801 (2018); L. Calibbi, A. Crivellin, and T. Li, *Physical Review D* **98**, 115002 (2018); A. Crivellin, D. Müller, and T. Ota, *Journal of High Energy Physics* **2017**, 1 (2017); A. Crivellin, C. Greub, F. Saturnino, and D. Müller, *Physical review letters* **122**, 011805 (2019); A. Crivellin, D. Müller, A. Signer, and Y. Ulrich, *Physical Review D* **97**, 015019 (2018); K. Babu, P. B. Dev, S. Jana, and A. Thapa, *Journal of High Energy Physics* **2021**, 1 (2021).
- [22] S. Weinberg, in *AIP Conference Proceedings*, Vol. 272 (American Institute of Physics, 1992) pp. 346–366.
- [23] S. Pastore, L. Girlanda, R. Schiavilla, M. Viviani, and R. Wiringa, *Physical Review C* **80**, 034004 (2009).
- [24] G. Panico, A. Pomarol, and M. Riembau, *Journal of High Energy Physics* **2019**, 1 (2019).
- [25] A. Dedes, M. Paraskevas, J. Rosiek, K. Suxho, and L. Trifyllis, *Journal of High Energy Physics* **2018**, 1 (2018); A. V. Manohar and M. B. Wise, *Physics Letters B* **636**, 107 (2006); C. Grojean, E. E. Jenkins, A. V. Manohar, and M. Trott, *Journal of High Energy Physics* **2013**, 16 (2013); M. Ghezzi, R. Gomez-Ambrosio, G. Passarino, and S. Uccirati, **2015**, 1 (2015); E. Vryonidou and C. Zhang, **2018**, 1 (2018); S. Dawson and P. P. Giardino, *Physical Review D* **97**, 093003 (2018).
- [26] M. Bilenky and A. Santamaria, *Nuclear Physics B* **420**, 47 (1994); M. Gell-Mann, P. Ramond, and R. Slansky, *Supergravity*, P. van Nieuwenhuizen and DZ Freedman ed., North Holland, Amsterdam, 315 (1979); T. Yanagida, *KEK Report No. 79-18* **95** (1979); P. W. Angel, N. L. Rodd, and R. R. Volkas, *Physical Review D* **87**, 073007 (2013); K. Babu and C. N. Leung, *Nuclear Physics B* **619**, 667 (2001); M. B. Krauss, T. Ota, W. Porod, and W. Winter, *Physical Review D* **84**, 115023 (2011).
- [27] M. Aaboud, G. Aad, B. Abbott, B. Abeloos, S. Abidi, O. AbouZeid, N. Abraham, H. Abramowicz, H. Abreu, R. Abreu, *et al.*, *Journal of High Energy Physics* **2017**, 1 (2017).
- [28] J. Alvarado, C. E. Diaz, and R. Martinez, *Physical Review D* **100**, 055037 (2019).
- [29] P. Z. et al. (Particle Data Group), *Progress of Theoretical and Experimental Physics* **2020** (2020), 10.1093/ptep/ptaa104,

- 083C01, <https://academic.oup.com/ptep/article-pdf/2020/8/083C01/34673722/ptaa104.pdf>.
- [30] A. Castro, arXiv preprint arXiv:1911.09437 (2019).
 - [31] R. Martinez, F. Ochoa, and J. Quimbayo, Physical Review D **98**, 035036 (2018).
 - [32] G. Buchalla and A. Buras, Rev. Mod. Phys **68**, 1125 (1996); G. Hiller and F. Krüger, Physical Review D **69**, 074020 (2004); C.-W. Chiang, X.-G. He, and G. Valencia, **93**, 074003 (2016).
 - [33] D. M. Straub, arXiv preprint arXiv:1810.08132 (2018).
 - [34] C.-W. Chiang, X.-G. He, and G. Valencia, Physical Review D **93**, 074003 (2016).
 - [35] G. D’Amico, M. Nardecchia, P. Panci, F. Sannino, A. Strumia, R. Torre, and A. Urbano, Journal of High Energy Physics **2017**, 1 (2017).
 - [36] J. Beringer *et al.*, Phys. Rev. D **86** (2012).
 - [37] J. Alvarado, M. Bulla, D. Martinez, and R. Martinez, arXiv preprint arXiv:2010.02373 (2020).
 - [38] J. Alvarado and R. Martinez, arXiv preprint arXiv:2007.14519 (2020).
 - [39] F. Jegerlehner and A. Nyffeler, Physics Reports **477**, 1 (2009).
 - [40] A. Miucci, C. Merlassino, S. Haug, J. K. Anders, H. P. Beck, A. Ereditato, G. A. A. Mullier, M. Rimoldi, and T. D. Weston, Journal of High Energy Physics **2019** (2019).